Received: 15 April 2023 | Revised: 12 January 2024 | Accepted: 16 January 2024

DOI: 10.1002/pld3.568

RESEARCH ARTICLE

Identification and expression of strigolactone biosynthesis and signaling genes and the in vitro effects of strigolactones in olive (*Olea europaea* L.)

Aslıhan Özbilen[1] | Fatih Sezer[2] | Kemal Melih Taşkin[2]

[1]Department of Biology, Canakkale Onsekiz Mart University, Canakkale, Turkey

[2]Department of Molecular Biology and Genetics, Canakkale Onsekiz Mart University, Canakkale, Turkey

Correspondence
Aslıhan Özbilen, Department of Biology, Canakkale Onsekiz Mart University, 17100 Canakkale, Turkey.
Email: aozbilen@comu.edu.tr

Funding information
COST Action, Grant/Award Numbers: FA12063, FA1206; Scientific and Technological Research Council of Turkey (TUBITAK), Grant/Award Number: 215O543

Abstract

Strigolactones (SLs), synthesized in plant roots, play a dual role in modulating plant growth and development, and in inducing the germination of parasitic plant seeds and arbuscular mycorrhizal fungi in the rhizosphere. As phytohormones, SLs are crucial in regulating branching and shaping plant architecture. Despite the significant impact of branching strategies on the yield performance of fruit crops, limited research has been conducted on SLs in these crops. In our study, we identified the transcript sequences of SL biosynthesis and signaling genes in olive (*Olea europaea* L.) using rapid amplification of cDNA ends. We predicted the corresponding protein sequences, analyzed their characteristics, and conducted molecular docking with bioinformatics tools. Furthermore, we quantified the expression levels of these genes in various tissues using quantitative real-time PCR. Our findings demonstrate the predominant expression of SL biosynthesis and signaling genes (*OeD27*, *OeMAX3*, *OeMAX4*, *OeMAX1*, *OeD14*, and *OeMAX2*) in roots and lateral buds, highlighting their importance in branching. Treatment with *rac*-GR24, an SL analog, enhanced the germination frequency of olive seeds in vitro compared with untreated embryos. Conversely, inhibition of SL biosynthesis with TIS108 increased lateral bud formation in a hard-to-root cultivar, underscoring the role of SLs as phytohormones in olives. These results suggest that modifying SL biosynthesis and signaling pathways could offer novel approaches for olive breeding, with potential applicability to other fruit crops.

KEYWORDS
GR24, olive, qPCR, strigolactones, TIS108, tissue culture

1 | INTRODUCTION

The olive (*Olea europaea* L.), a commercially significant crop in the Mediterranean region, is renowned for its fruits, which are utilized for both table consumption and oil production. As one of the oldest cultivated trees, it holds a prominent place in agricultural history (Rugini, 1986; Zohary et al., 2012). Olive production represents a vital agricultural industry with substantial economic potential. However, classical breeding programs for olives are notably time-consuming (Fabbri et al., 2009). Consequently, the tree's branching structure is of particular importance for propagation and yield. While numerous studies have focused on the physiological aspects of olives, such as

the fatty acids and phenolic compounds in olive oil, fruits, or leaves (Ballus et al., 2014; Scoditti et al., 2014; Talhaoui et al., 2015), there is a notable gap in the literature regarding the molecular mechanisms underlying olive branching.

Strigolactones (SLs), a class of compounds derived from carotenoids, function dually as signaling molecules and endogenous phytohormones. In the rhizosphere, SLs are detected by the seeds of parasitic plants, triggering germination (Cook et al., 1966), and by arbuscular mycorrhizal fungi, facilitating symbiosis (Akiyama et al., 2005; Fiorilli et al., 2019). Additionally, SLs are pivotal in controlling plant architecture; they suppress lateral bud formation and shoot branching (Gomez-Roldan et al., 2008; Umehara et al., 2008). Beyond these roles, SLs contribute to the increase in internodal distance and stem elongation (de Saint Germain et al., 2013; Guan et al., 2012), regulate leaf senescence (Snowden et al., 2005; Van Dingenen et al., 2023; Yamada et al., 2014), and are involved in transverse thickening (Agusti et al., 2011). Furthermore, SLs influence leaf morphology (Stirnberg et al., 2002) and exhibit a positive response to environmental stresses such as drought, cold, salt, and heavy metal exposure (Ha et al., 2014; Tai et al., 2017; Wang et al., 2023).

SLs possess a tricyclic lactone structure composed of A-, B-, and C-rings, coupled with a butenolide (D-ring) via an enol ether bond. The D-ring is predominantly regarded as essential for SLs' biological activity (Umehara et al., 2015). SLs that contain complete ABC rings and a D-ring are classified as canonical SLs, whereas those with incomplete ABC rings but still retaining a D-ring are termed non-canonical SLs (Al-Babili & Bouwmeester, 2015; Yoneyama, Mori, et al., 2018).

Primarily synthesized in the roots, SLs are translocated to the aerial parts of the plant (Booker et al., 2005) (Figure 1). The biosynthetic pathway of SLs initiates in the plastids with an isomerization reaction, followed by several cleavage steps. Initially, all-*trans*-β-carotene undergoes isomerization to 9-*cis*-β-carotene catalyzed by the DWARF27 (D27) enzyme (Alder et al., 2012). Subsequently, CCD7 (carotenoid cleavage dioxygenase 7/MAX3—more axillary growth 3) cleaves 9-*cis*-β-carotene into 9-*cis*-β-apo-10′-carotenal (Booker et al., 2004; Chen, Wang, et al., 2022), which is then transformed into carlactone by CCD8 (carotenoid cleavage dioxygenase 8/MAX4—more axillary growth 4) (Alder et al., 2012; Schwartz et al., 2004; Seto et al., 2014). In the subsequent step, a cytochrome P450 enzyme, coded by *MAX1* (*more axillary growth 1*), converts carlactone to 5-deoxy-strigol in the cytoplasm. MAX1 is first identified for *Arabidopsis thaliana* (Booker et al., 2005). Recent studies also revealed that MAX1 homologs can also convert carlactone to carlactonic acid, to 4-deoxyorobanchol, to orobanchol, or to methyl carlactonoate (Abe et al., 2014; Brewer et al., 2016; Chen, Song, et al., 2023; Cui et al., 2023; Ito et al., 2022; Yoneyama, Xie, et al., 2018; Zhang et al., 2014).

In plants, SL perception involves a series of enzymatic interactions. DWARF14 (D14), an α/β hydrolase protein, facilitates the hydrolytic cleavage of the D-ring of SLs (Arite et al., 2009), resulting in the formation of a D14/D-ring complex. After this step, a suppressor protein binds the complex and blocks SL signaling (Jiang et al., 2013; Zhou et al., 2013). Later, MAX2 (More Axillary Branches 2), as a member of the SCF (S-phase kinase-associated protein (Skp)1–Cullin–F-Box)-ubiquitin complex, catalyzes ubiquitination of the suppressor protein and initiates the SL signaling (Jiang et al., 2013; Zhou et al., 2013).

Because the production via seeds is a long and slow process, olive is mostly propagated via cuttings in a moist environment (Fabbri et al., 2004). However, some agriculturally important olive cultivars can only be propagated by inoculation because their rooting capacities are very limited (Çetintaş Gerakkakis & Özkaya, 2005). Ayvalık olive cultivar is an easy-to-root (ER) cultivar and one of the most common cultivars grown in Turkey for olive oil, while Domat, which bears large fruits, is a hard-to-root (HR) cultivar and traditional plant growth regulator (PGR) applications (such as indole butyric acid) are insufficient for inducing rooting.

In this study, we conducted molecular characterization and bioinformatic analysis of the SL biosynthesis (*OeD27*, *OeMAX3*, *OeMAX4*, and *OeMAX1*) and signaling genes (*OeD14* and *OeMAX2*). We determined the expression levels of these genes in various tissues of the "Ayvalık" and "Domat" olive cultivars, including apical buds, lateral buds, leaves, and roots for "Ayvalık," and the basal portion of the cuttings for "Domat," where root samples were unobtainable. This analysis of SL genes in olive aims to shed light on the molecular mechanisms of shoot branching in woody plants. Furthermore, we examined the impacts of *rac*-GR24, an SL analog, and TIS108, an SL biosynthesis inhibitor, on "Ayvalık" (ER) and "Domat" (HR) olive explants under in vitro conditions. Under tissue culture conditions, we assessed seed and embryo germination rates, root lengths, lateral

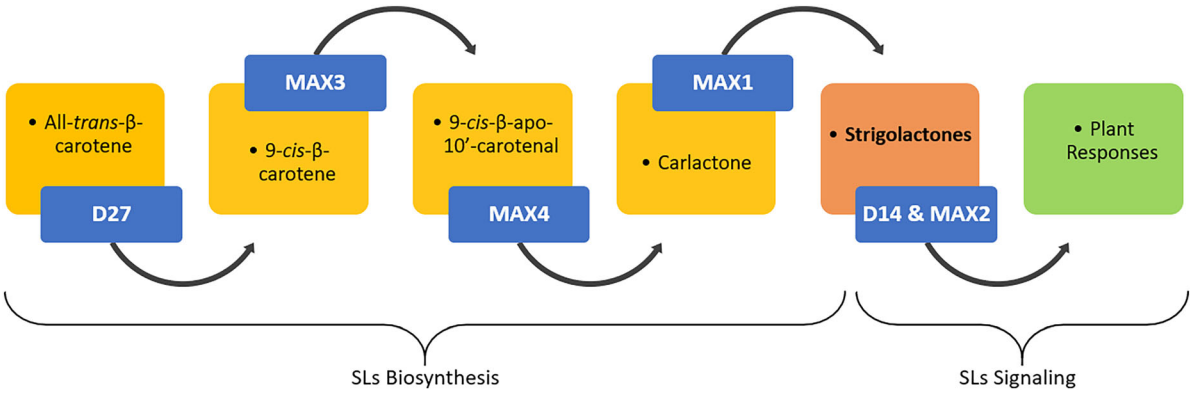

FIGURE 1 Strigolactone biosynthesis and signaling pathway (based on Czarnecki et al., 2013).

branching, and internode lengths, using both MS and olive media supplemented with various concentrations of *rac*-GR24 and TIS108. Notably, TIS108, a triazole-type inhibitor, selectively targets cytochrome P450 proteins like MAX1s (Ito et al., 2013; Ito et al., 2022). The effects of these PGRs were also investigated on nodal explants cultured in vitro.

While the majority of SL studies use model organisms such as rice or *A. thaliana*. However, little is known about SLs in fruit crops in which control of branching is one of the most important agricultural characteristics. This study demonstrates that SL biosynthesis and signaling genes are conserved in woody perennials, thereby offering new tools for breeding and cultivation strategies that leverage SL biosynthesis and signaling mechanisms in fruit crops.

2 | MATERIALS AND METHODS

2.1 | Plant material and RNA isolation

SL biosynthesis primarily occurs in roots (Booker et al., 2005). For our study, we obtained conventionally grown 2-month-old "Ayvalık" and "Domat" cuttings from the Edremit Directorate of Olive Production Station (Edremit, Balıkesir). Fresh roots from the "Ayvalık" cuttings were collected. For the "Domat" cultivar, owing to its HR nature, we collected only the basal portion of the cuttings (approximately .5 cm from the base) as described by Porfirio et al. (2016). Additionally, apical buds, lateral buds, and leaves from three different trees of each cultivar were collected. Total RNA isolation from these tissues was performed using the Purelink RNA Mini Kit (Invitrogen—12183018A) and TRIzol® Reagent (Thermo Fischer—15596026). The quantities of RNA were measured with a Qubit 2.0 (Thermo Fischer) fluorometer, and band integrities were checked with agarose gel electrophoresis.

2.2 | Primer design

Gene-specific primers for RACE and expression studies were designed using Geneious R8 (Kearse et al., 2012). Initially, partial transcript reads of olive were downloaded from available databases (NCBI [National Center for Biotechnology Information], Phytozome) and then imported into Geneious R8. The design of olive-specific primers was guided by the following criteria: GC content between 40% and 60%, melting temperature (Tm) between 57 and 63°C, primer length between 18 and 27 base pairs (bp), and for real-time PCR studies, a product size between 80 and 150 bp. Additionally, for RACE studies, multiple primers were selected for each gene to ensure specific and accurate amplification (refer to Tables S1–S4 and Figure S1).

2.3 | RT-PCR studies of RACE

We employed classical RACE protocols to amplify the 3′ and 5′ ends of the "Ayvalık" transcripts (Scotto-Lavino et al., 2006a, 2006b). For 3′ ends, cDNA was synthesized using an oligo-dT adapter primer (5′-CCAGTGAGCAGAGTGACGAGGACTCGAGCTCAAGCTTTTTTTTTTTTTTT-3′), and for 5′ ends, cDNA synthesis was conducted with GSP1 (Gene Specific Primer1) for each gene. Utilizing 5 µg of DNase-treated total RNA (DNase I, RNase-free—Thermo Fischer Scientific—EN0525), cDNA was synthesized following the instructions of the High-Capacity cDNA Reverse Transcription Kit (Applied Biosystems, 4368814). Although oligo-dT-derived cDNA is ready for 3′ end studies, additional steps were required for GSP1-derived cDNAs for 5′ ends. These cDNAs were purified (Scotto-Lavino et al., 2006b) using the GeneJET PCR Purification Kit (Thermo Fischer, K0701) and subsequently treated with terminal transferase (Terminal Deoxynucleotidyl Transferase, Thermo Fischer, EP0161) to add a polyA tail. The resulting cDNA templates were diluted to 1 mL with Tris-EDTA (pH 8.0) buffer and stored at 4°C until use.

At least two rounds of RT-PCR were performed for 3′ or 5′ RACE using 1 µL of the cDNA templates. The first PCRs for 3′ RACE employed GSP1 and adapter primers (5′–CCAGTGAGCAGAGTGACG–3′ and/or 5′–GAGGACTCGAGCTCAAGC–3′). The first PCR products were then used in nested PCRs with GSP2, GSP3, or GSP4 primers to identify the specific product of interest. For 5′ RACE, the first PCRs used GSP2 and oligo-dT adapter primers, followed by a second round of amplification with adapter primers and GSP3 or GSP4, using the first PCR products as templates.

The first round of RT-PCRs included an initial denaturation step at 98°C for 5 min, followed by annealing at 54–62°C for 30 s, and an elongation step at 72°C for 40 min for synthesis efficiency (Scotto-Lavino et al., 2006a). Subsequent RT-PCRs involved 36 cycles of 98°C for 30 s, 54–62°C for 30 s, 72°C for 30 s/kb, and a final extension at 72°C for 10 min. The conditions for the second or third nested RT-PCRs were similar. RT-PCRs were executed with Phusion High Fidelity DNA Polymerase (Thermo Scientific, F530L) and products were verified by 1% agarose gel electrophoresis. The accurate bands for each gene were extracted from the gel using the PureLink® Quick Gel Extraction Kit (K210012) and sequenced (Macrogen-Netherlands and Medsantek-Turkey).

After acquiring the 3′ and 5′ ends, the interior parts of the transcripts were also amplified. Primers for these regions were selected using Geneious R8, and the PCR products were sequenced (Macrogen, Netherlands, and Medsantek, Turkey). Sequence reads were analyzed in Geneious R8 (Kearse et al., 2012). Transcripts were filtered and trimmed with a .05 error limit based on their quality scores. The filtered and trimmed reads were mapped to the reference sequence (Sylvestris) for each gene. After assembly, consensus transcript sequences were compared against sequences from other plant species using BLASTn in NCBI. Putative protein sequences were also predicted from these transcripts.

2.4 | Bioinformatic studies

To identify the orthologs of SL biosynthesis and signaling genes, we employed the BLASTp algorithm in Geneious R8 (Kearse et al., 2012).

Sequences with high similarity scores from other well-known plant species, including olive "Sylvestris" and "Arbequina" cultivars, were selected (Rao et al., 2021; Ünver et al., 2017). These protein sequences were aligned using the MUSCLE algorithm (Edgar, 2004) in Geneious R8, adhering to the default parameters. Following alignment, phylogenetic trees were constructed for each gene using the UPGMA algorithm in Geneious R8.

In addition, the molecular weights and isoelectric points (pI) of the "Ayvalık" putative proteins were estimated using the ProtParam tool on the ExPASy portal (https://web.expasy.org/protparam/; Gasteiger et al., 2005). Subcellular localizations were predicted with DeepLoc-1.0 (https://services.healthtech.dtu.dk/services/DeepLoc-1.0/; Almagro Armenteros et al., 2017), and conserved domain analysis was performed using the InterPro tool (https://www.ebi.ac.uk/interpro/; Mitchell et al., 2019).

Understanding the binding mechanisms between ligands and receptors at the molecular level helps researchers comprehend the structural basis of biological processes. Therefore, we performed molecular docking experiments with the OeD14 protein by using AutoDock Vina (Trott & Olson, 2010) to show the interaction between OeD14 and *rac*-GR24 bioinformatically. To achieve our objective, we initially acquired 3D conformer structures of 15 different SL molecules (4-deoxyorobanchol, 5-deoxystrigol, Avenaol, Carlactone, Carlactonic acid, Heliolactone, Medicaol, Orobanchol, *rac*-GR24, Solanacol, Sorgolactone, Sorgomol, Strigol, Strigone, and Zealactone) from PubChem (https://pubchem.ncbi.nlm.nih.gov/) in SDF (Structure-Data Files) format. For ligand preparation for docking, these SDF formatted SL files were converted into PDB (Protein Data Bank) and subsequently into PDBQT (a modified PDB format which includes atomic charges and atom types) format using PyMOL (https://pymol.org/2/) and AutoDock Vina, respectively. We then acquired the 3D structure of OeD14 using SWISS-MODEL (Waterhouse et al., 2018) in PDB format, which was validated using VERIFY 3D (Lüthy et al., 1992). Water molecules were removed from the protein structure, polar hydrogen atoms and Kollman charges were added using AutoDock Vina, and the protein was saved in PDBQT format. Following the preparation of both ligands and the protein, blind docking of all ligands against OeD14 was performed. Grid dimensions for the docking were set to 126, 126, 126 in x, y, and z axes, with the center grid box coordinates at −16.516, 57.569, and −19.332 for x, y, and z, respectively. Post-docking, results were visualized using BIOVIA Discovery Studio (https://discover.3ds.com/discovery-studio-visualizer-download).

Being a member of the α/β hydrolase superfamily, D14 proteins possess a highly conserved catalytic Ser-Asp-His triad, essential for hydrolase activity (Nakamura et al., 2013). To this end, we retrieved D14 protein sequences of rice, poplar, *A. thaliana*, petunia, and tomato from the NCBI database (XP_015631400.1, XP_002302409.1, NP_566220.1, J9U5U9.1, and XP_004238093.1, respectively). These sequences were aligned with the "Ayvalık" cultivar protein sequence using the MUSCLE algorithm in Geneious software, highlighting the conserved catalytic triad.

In addition to docking, we performed 3D modeling studies to compare *A. thaliana* and *O. europaea* SL biosynthesis and signaling protein structures. We obtained *A. thaliana* protein sequences from The Arabidopsis Information Resource (TAIR) and *O. europaea* SL protein sequences from the NCBI database. We used the SWISS-MODEL (https://swissmodel.expasy.org, Waterhouse et al., 2018) tool with default parameters.

Furthermore, we analyzed 1500 bp upstream of the genomic sequences for promoter analysis. Investigating promoter regions offers crucial insights into the mechanisms governing gene expression and hormone receptor interactions, predominantly through transcription factors. To this end, we used *A. thaliana* genomic sequences as a reference and sourced annotated genomic data of wild olive (*O. europaea var. Sylvestris*) from Ünver et al. (2017). We isolated the 1500 bp region upstream of the first exon for each gene. The regulatory elements in these promoter regions were identified using the PlantCARE tool (http://bioinformatics.psb.ugent.be/webtools/plantcare/html/; Lescot et al., 2002).

2.5 | Gene expression studies

We examined the expression profiles of genes responsible for the biosynthesis and signaling of SLs (*OeMAX1*, *OeMAX2*, *OeMAX3*, *OeMAX4*, *OeD14*, and *OeD27*) in the Ayvalık and Domat olive cultivar tissues using the Real-Time PCR SYBR Green I method. The tissues, including roots/basal portion of the cuttings, leaves, apical buds, and lateral buds, were collected from three different trees/seedlings at the Edremit Directorate of Olive Production Station (Edremit, Balıkesir). RNA was isolated from these biological replicates, and cDNA was synthesized with random primers as per the manufacturer's instructions (High-Capacity cDNA Reverse Transcription Kit, Applied Biosystems, 4368814).

Primers for these genes were selected using olive transcripts with the Geneious R8 software (Kearse et al., 2012). Initially, the efficiency of each primer pair was assessed. For this, we prepared a serial dilution (1, 1:10, 1:100, 1:1000, 1:10000, and 1:100000) of a pooled cDNA sample (comprising root, leaf, and bud tissues) for each primer pair. The qPCR reactions were conducted using these cDNAs, specific primer pairs, and SYBR Green Master Mix (Power SYBR Green PCR Master Mix, 1604522). Three technical replicates were performed, and standard curves were constructed using the mean CT (threshold cycle) values of each primer pair in Excel. The slope of the curve and the correlation coefficient were calculated, and the reaction efficiency for each primer pair was determined using the formula: $(10^{(-1/\text{slope})} - 1) \times 100$. Primers with an efficiency between 90% and 110% were selected for qPCR reactions. Each expression study included three biological and technical replicates. The PCR conditions were set to 10 min at 95°C, followed by 40 cycles of 15 s at 95°C, 1 min at 60°C, and 1 min at 72°C. Melt curve analysis was performed to ensure product specificity. Negative RT control reactions without reverse transcriptase and negative controls without cDNA template were also included. Normalization of the reactions was performed

using *UBC1 (Ubiquitin-conjugating enzyme)* and *CLATHRIN* (Clathrin adaptor complex medium subunit) primers, as described in our previous study (Hürkan et al., 2018). Results of relative gene expression were analyzed according to the methods of Pfaffl (2001, 2004) and Vandesompele et al. (2002).

2.6 | Tissue culture studies

For tissue culture, plant materials from the ER "Ayvalık" cultivar (ER) and HR "Domat" cultivar (HR) were obtained from the Edremit Olive Production Station Directorate (Edremit/Balıkesir/Turkey). Olive fruits were manually harvested from trees in October 2018 (Figure 2a). After removing the exocarp, fleshy mesocarp, and stony endocarps, the seeds were extracted (Figure 2b). These seeds underwent a sterilization process, initially treated with 70% ethanol for 1 min and subsequently with 20% (v/v) commercial bleach for 20 min. Following this, the seeds were rinsed three times with sterile water and soaked overnight in sterile distilled water. The sterilization steps were repeated the next day. The surface-sterilized seeds were then aseptically placed in Petri dishes containing MS medium (Murashige & Skoog, 1962) supplemented with .8% (w/v) agar and 3% (w/v) mannitol (D-Mannitol, Duchefa, M0803) (Garcia et al., 2002; Leva et al., 1994) and PGRs. Each group initially started with 50 seeds/embryos (n), though this number decreased over time in some groups due to contamination. Nevertheless, a minimum of five individuals per group was maintained for statistical analysis. We cultured whole seeds and embryos without testa and endosperm, as endosperm has been reported to delay germination in some olive cultivars (Voyiatzis, 1995) (Figure 2c–e). The growth regulators (*rac*-GR24 and TIS108), dissolved in DMSO and filter sterilized, were added to the medium after autoclaving. Explants were subcultured every 4–8 weeks in a laminar flow hood.

The effects of *rac*-GR24 and TIS108 at various concentrations (1, 5, and 10 μM) were evaluated based on previous studies on different plant species (Hamiaux et al., 2012; Ruyter-Spira et al., 2011), including control groups without PGRs. The explants underwent vernalization at 10°C for 4 weeks in the dark, then transferred to a plant growth chamber at 21°C with a 16/8 h light/dark photoperiod under white fluorescent light to initiate germination. After 4 weeks in culture, germination frequencies for PGR treatments were determined, and root lengths were measured (Figure 2f). Subsequently, the explants were transferred to magenta vessels under the same conditions (Figure 2g) for another month, followed by transfer to pots containing a peat/perlite mixture (3:1 v/v) in a growth chamber for an additional 4 months (Fabbri et al., 2004) (Figure 2h). At the end of the 6-month culture period, to assess the effects of *rac*-GR24 and TIS108 on olive explants, the number of lateral branches and internode lengths were measured (Figure 2i,j).

The variations in germination frequency and the number of lateral branches between PGR treatments were analyzed and graphics were generated in Excel. Statistical analyses for germination, lateral branches, and shoot growth percentages are done with the Kruskal–Wallis test followed by Dunn's post hoc test with Bonferroni correction at $p < .05$ level of significance, statistics for root and internode lengths were performed using the one-way analysis of variance (ANOVA) test followed by Tukey's post-test at $p < .05$ level of significance, and statistics for gene expression data were done for each tissue of two cultivars with independent-samples *t*-test at $p < .05$ level of significance in the SPSS (Statistical Package for the Social Sciences, v27) program.

We also evaluated the impact of *rac*-GR24 and TIS108 on olive nodal explants used for micropropagation. The nodal explants were sourced from 1-year-old trees of both the ER and HR cultivars (Figure 3a). For each PGR treatment group, 16 nodal explants underwent surface sterilization. Initially, the explants were cleansed under running water for 2 h, followed by sterilization using 20 mg/L carbendazim (50%) for 30 min, 10% sodium hypochlorite, and .035% $HgCl_2$ for 5 min. Subsequently, the explants were rinsed three times with sterile distilled water before being transferred to olive medium (OM) containing .4% (w/v) mannitol, 3% (w/v) agar, and .8% (w/v). Each explant was placed in an individual tube measuring 25 mm in diameter and 150 mm in length. Sterilized solutions of *rac*-GR24 and TIS108 were added to the mediums in three concentrations (1, 5, and 10 μM) post-sterilization. Zeatin (2 mg/L) served as a positive control for lateral bud growth in each cultivar, while OM0 medium without any PGRs was used as the negative control.

3 | RESULTS

3.1 | Full-length cDNAs of SL biosynthesis and signaling genes revealed by RACE studies

To ascertain the full-length mRNA sequences, we conducted RACE studies for each gene. The 3′ and 5′ ends of the transcripts were amplified through a series of PCR steps. Initially, we amplified large fragments of the transcripts using outer primers. Subsequently, using the initial PCR products as templates and nested primers, the 3′ and 5′ ends of the olive transcripts were amplified through additional rounds of PCR. The PCR products, extracted from agarose gels, were sequenced. The resulting reads were then assembled to the reference sequence. The consensus sequence lengths for olive SL biosynthesis and signaling genes ranged from 801 to 2262 bp (Table 1). These consensus sequences were submitted to the NCBI database. Additionally, we compared the identities of these sequences via BLASTn analysis with those from the wild olive (*Sylvestris* cultivar) and *A. thaliana* (Table 1).

3.2 | Phylogenetic analyses of putative proteins show a conserved mechanism for the SL biosynthesis and signaling genes

We aligned the putative olive protein sequences with those of other plant species and constructed phylogenetic trees (Figures S2–S7). In

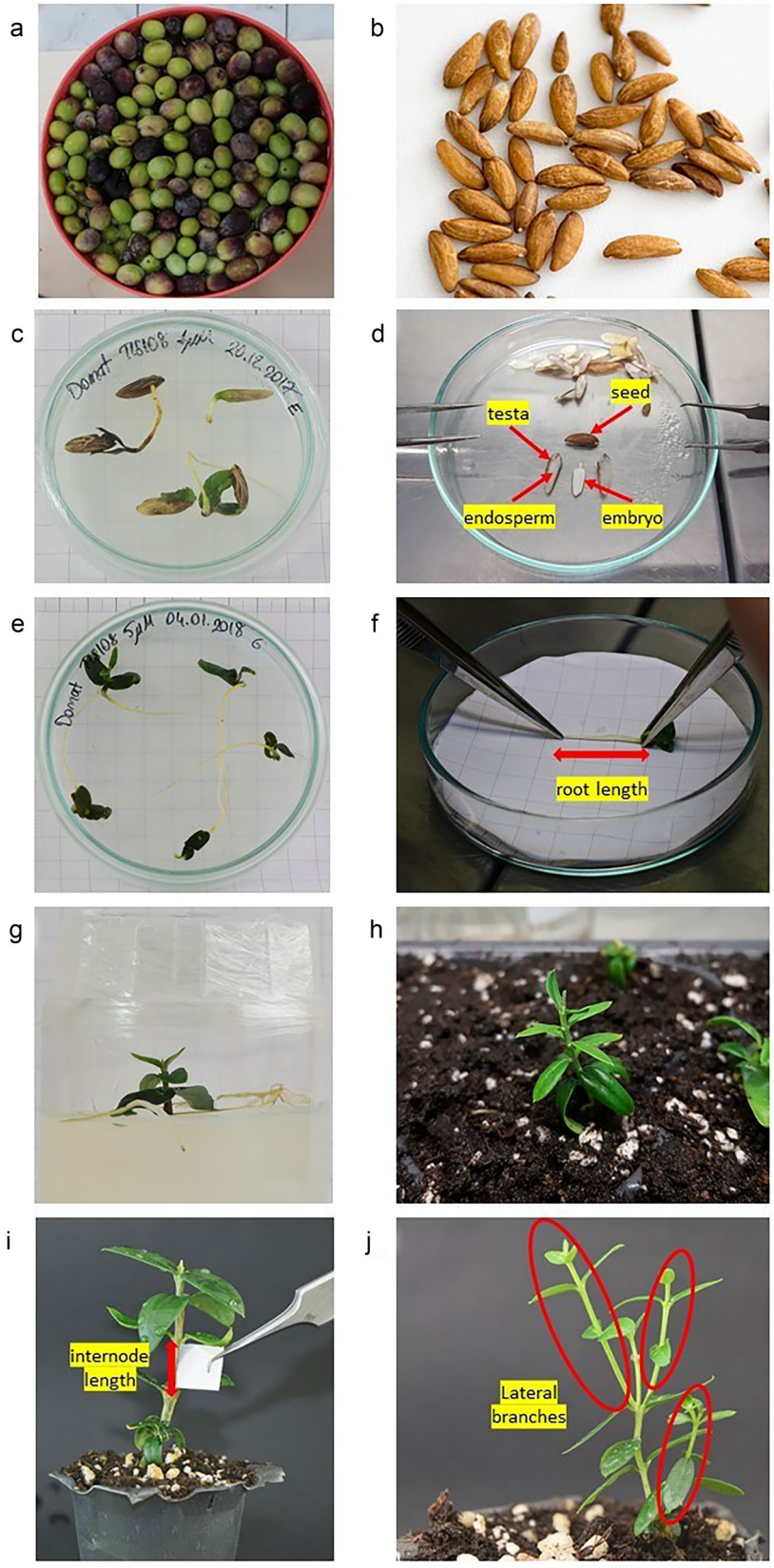

FIGURE 2 (a) Olive fruits collected manually from trees. (b) Seeds without exocarp, fleshy mesocarp, and the stony endocarp. (c) Olive seedlings derived from seeds, after 4 weeks in culture. (d) Embryos without testa and the endosperm. (e) Seedlings derived from embryos, after 4 weeks in culture. (f) The measurements of root lengths, after 4 weeks in culture. (g) Seedlings sub-cultured in magenta vessels every 4–8 weeks in culture. (h) 2–6 months old seedlings grown in pots containing a peat/perlite mixture. (i) The measurements of internode lengths. (j) The number of lateral branches in 6-month-old olive plants.

these trees, the sequences of the "Ayvalık" olive cultivar clustered closely with those of the "Sylvestris" and "Arbequina" cultivars. Specifically, the SL biosynthetic and signaling proteins from "Sylvestris" (XP_022854732.1, XP_022898986.1, XP_022862522.1, XP_022855437.1, XP_022870880.1, and XP_022872511.1) showed close relationships with the "Ayvalık" proteins *OeD27* (QMX78398.1),

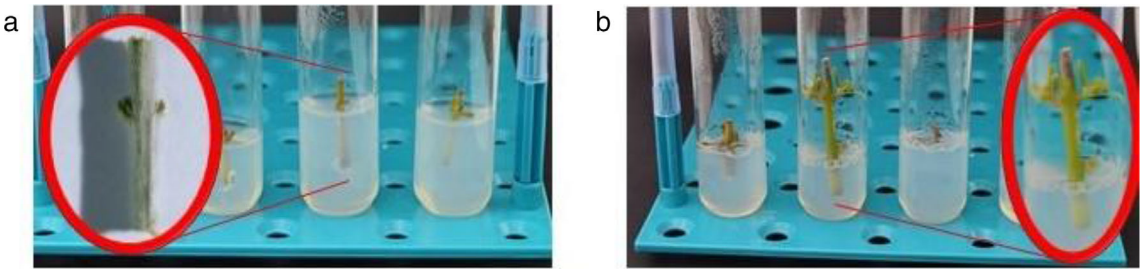

FIGURE 3 (a) Nodal explants aseptically cultured in olive medium. (b) Formation of lateral buds after 4 weeks in culture.

TABLE 1 Transcript information of olive "Ayvalık" obtained from RACE studies.

	Total reads	Consensus sequence (bp)	NCBI accession number	Identity to Sylvestris cultivar	Identity to *Arabidopsis thaliana*
D27	9	801	MN917100	99%	70%
MAX3	13	1881	MN917103	99%	68%
MAX4	9	1603	MN917104	99%	68%
MAX1	8	1688	MN917101	99%	70%
D14	8	1013	MN917099	100%	70%
MAX2	11	2262	MN917102	99%	71%

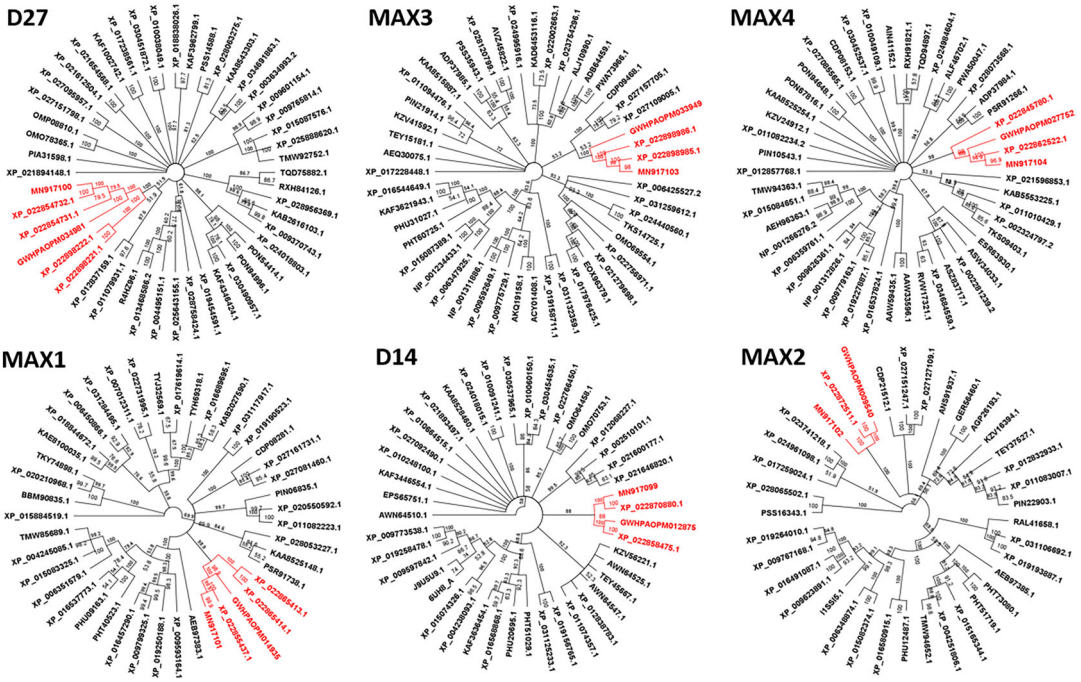

FIGURE 4 Phylogenetic trees of strigolactone (SL) proteins (red branches show olive proteins including putative Ayvalık cultivar protein sequences).

OeMAX3 (QMX78401.1), *OeMAX4* (QMX78402.1), *OeMAX1* (QMX78399.1), *OeD14* (QMX78397.1), and *OeMAX2* (QMX78400.1), respectively. These phylogenetic trees indicate that SL biosynthesis and signaling mechanisms are conserved among olive cultivars and across known plant species (Figure 4).

3.3 | SL protein characteristics are conserved in olive

Further bioinformatic analysis employing various tools delineated the biochemical properties (molecular weight, isoelectric points, and

subcellular localizations) of the predicted proteins (Table 2). The results indicate that the amino acid lengths of the olive proteins are similar to those of *A. thaliana*, and they share conserved domains. The subcellular localizations of these proteins were consistent with their functional roles.

According to our docking results, the binding affinities of the ligands to the OeD14 protein ranged from −4.8 to −7.0 Kcal/mol (Table S5). Ligands such as 4-deoxyorobanchol, 5-deoxystrigol, Avenaol, Medicaol, *rac*-GR24, Solanacol, Strigol, and Strigone exhibited lower binding affinity values (<−6.5 Kcal/mol) with OeD14, suggesting stronger interactions. Notably, only four of these ligands—4-deoxyorobanchol, 5-deoxystrigol, Medicaol, and *rac*-GR24—interact with the SL D-ring, implying that OeD14 can interact with both natural and synthetic SLs.

In the olive, the position of the catalytic triad was identified at Ser:96—Asp:217—His:246, and this configuration was conserved (Figure 5). The catalytic triad is situated within the central deep pocket of D14 proteins (Kagiyama et al., 2013). The conserved position of the catalytic triad in the olive protein and the bioinformatic docking site of *rac*-GR24 with OeD14, where the D-ring interacts with the asparagine residue at the 156th position, are depicted in Figure S8.

When we compared *A. thaliana* and *O. europaea* SL biosynthesis and signaling protein structures, we observed that the 3D structures of these proteins were highly similar, indicating the conservation of SL biosynthesis enzymes among plants (Table S6).

3.4 | Promoter analysis suggests a crosstalk between SLs and other plant hormones in olive

The upstream regions, extending 1500 bp from the start codon, were analyzed to identify regulatory promoter elements for each gene using the PlantCARE tool. We identified 70 different *cis*-acting elements predominantly related to environmental stress, light, and hormone responses.

The abscisic acid response element (ABRE) was present in all the investigated promoter regions. Additionally, a second ABRE element, ABRE4, was detected in the promoter regions of *OeMAX4*, *OeD14*, and *OeD27*. Gibberellin-responsive elements were also identified: the

TABLE 2 Characteristics of "Ayvalık" putative strigolactone (SL) proteins.

	Amino acid length (aa)	Molecular weight (Da)	Theoretical pI	Subcellular localization	Conserved domain	Identity to *Arabidopsis thaliana*
D27	253	28,954.92	9.05	Plastid	Cytochrome β-carotene isomerase D-27 like	41.5%
MAX3	437	50,273.14	8.88	Plastid	Cytochrome carotenoid oxygenase	62.2%
MAX4	418	46,233.77	5.74	Plastid	Cytochrome carotenoid oxygenase	70.6%
MAX1	449	50,632.59	9.14	Peroxisome	Cytochrome P450 superfamily	73.1%
D14	266	29,345.75	6.11	Cytoplasm	α/β hydrolase_1 superfamily	76.6%
MAX2	677	76,032.85	5.40	Nucleus	Leucine-rich repeat domain superfamily	52.6%

FIGURE 5 The alignment of homologous proteins of rice (*Oryza sativa*), *Populus trichocarpa*, *Arabidopsis thaliana*, petunia, and tomato (*Solanum lycopersicum*) with the olive (*Olea europaea*) Ayvalık cultivar protein. The red dots indicate the conserved amino acids of the Ser-Asp-His catalytic triad.

GARE-motif in *OeMAX1* and *OeD14*; the P-BOX in *OeMAX3*, *OeMAX4*, and *OeD14*; and the TATC-BOX in the *OeD14* promoter region.

The TCA-element, associated with salicylic acid responsiveness, was found in the promoter regions of *OeMAX1*, *OeMAX2*, and *OeMAX4*. In terms of auxin responsiveness, the TCA motif was detected in *OeMAX1*, *OeMAX4*, and *OeD14*, while another auxin-responsive element, the TGA-element, was found in *OeMAX3*, *OeMAX4*, and *OeD14*. Additionally, the TGACG motif, which is indicative of methyl jasmonate responsiveness, was present in the promoter regions of *OeMAX1*, *OeMAX3*, *OeMAX4*, *OeD14*, and *OeD27*.

3.5 | Expression of SL biosynthesis and signaling genes is primarily determined in roots/lateral buds

The expression levels of olive SL biosynthesis and signaling genes (*OeMAX1*, *OeMAX2*, *OeMAX3*, *OeMAX4*, *OeD14*, and *OeD27*) in various tissues, including roots/basal portion of the cuttings, leaves, apical buds, and lateral buds, were investigated using quantitative real-time PCR. In this study, primer pairs with efficiencies ranging from 92.5% to 99.4% were used (Figures S9–S14), and melt curve analysis confirmed the presence of a single PCR product (Figure S15).

We observed that the expression levels of OeSL biosynthetic genes (*OeD27*, *OeMAX3*, *OeMAX4*, and *OeMAX1*) were higher in the roots of the ER cultivar compared with other tissues (Figure 6). Additionally, for the HR cultivar, *MAX3* and *MAX4* showed higher expression in the basal portion of the cuttings. These findings suggest that SL biosynthesis primarily occurs in the roots of olive trees. Moreover, the expression levels of these SL biosynthesis genes in the root/basal portion of the cutting tissues were significantly lower in the HR cultivar compared with ER.

The OeSL perception and signaling genes, *OeD14* and *OeMAX2*, were expressed in all the examined tissues. *OeD14*, encoding an α/β hydrolase involved in SL perception, and *OeMAX2*, a member of the SCF-ubiquitin complex, exhibited higher expression in lateral buds compared with other tissues in both cultivars (Figure 7). This indicates that OeSL perception and signaling mainly occur in lateral buds. Furthermore, significant differences in SL signaling gene expression were only observed in the leaf tissues between the ER and HR cultivars.

3.6 | rac-GR24 and TIS108 have cultivar specific effects and can be used for propagation of some hard-to-root olive cultivars in tissue culture conditions

In vitro experiments were conducted to determine the effects of *rac*-GR24 (a synthetic SL) and the SL inhibitor TIS108 on the germination and development of seeds and plants. Doses of 1, 5, and 10 μM were

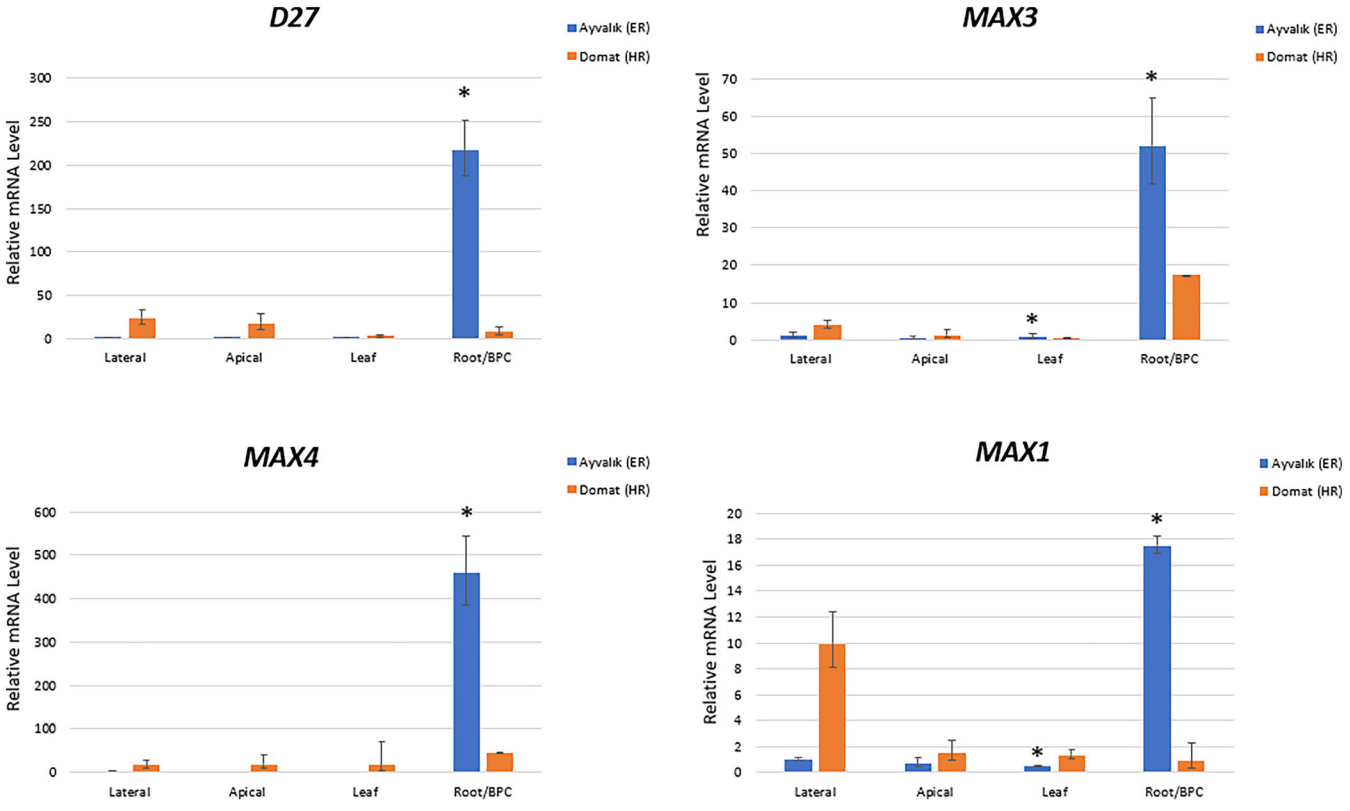

FIGURE 6 Quantitative real-time PCR expression profiles of olive strigolactone (SL) biosynthesis genes in apical and lateral buds, leaves, and roots of easy-to-root (ER)/the basal portion of the cuttings (BPC) of hard-to-root (HR). The statistical significance is determined by the independent-samples *t*-test at $p < .05$ level of significance (*) for each tissue of two cultivars, and error bars represent the standard error of the mean.

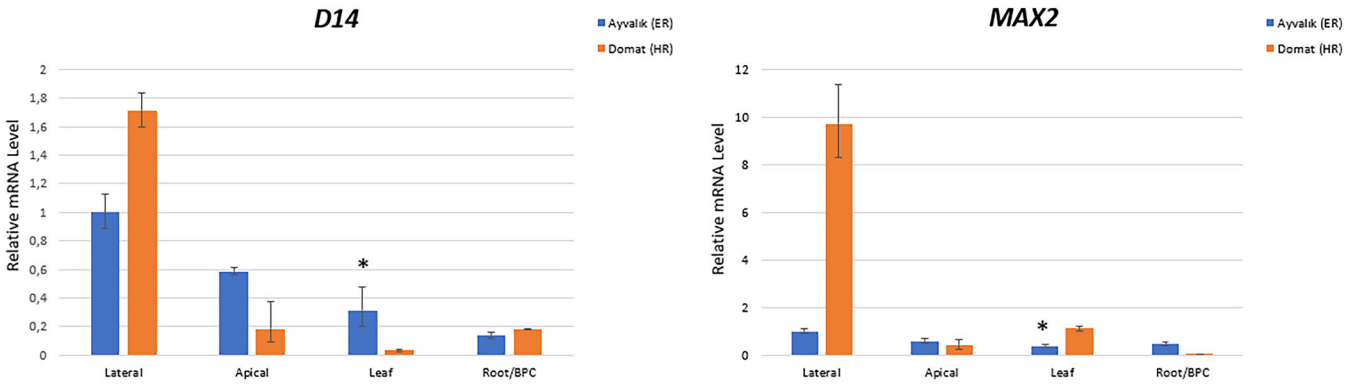

FIGURE 7 Quantitative real-time PCR expression profiles of olive strigolactone (SL) signaling genes in apical and lateral buds, leaves, and roots of easy-to-root (ER)/the basal portion of the cuttings (BPC) of hard-to-root (HR). The statistical significance is determined by the independent-samples *t*-test at $p < .05$ level of significance (*) for each tissue of two cultivars, and error bars represent the standard error of the mean.

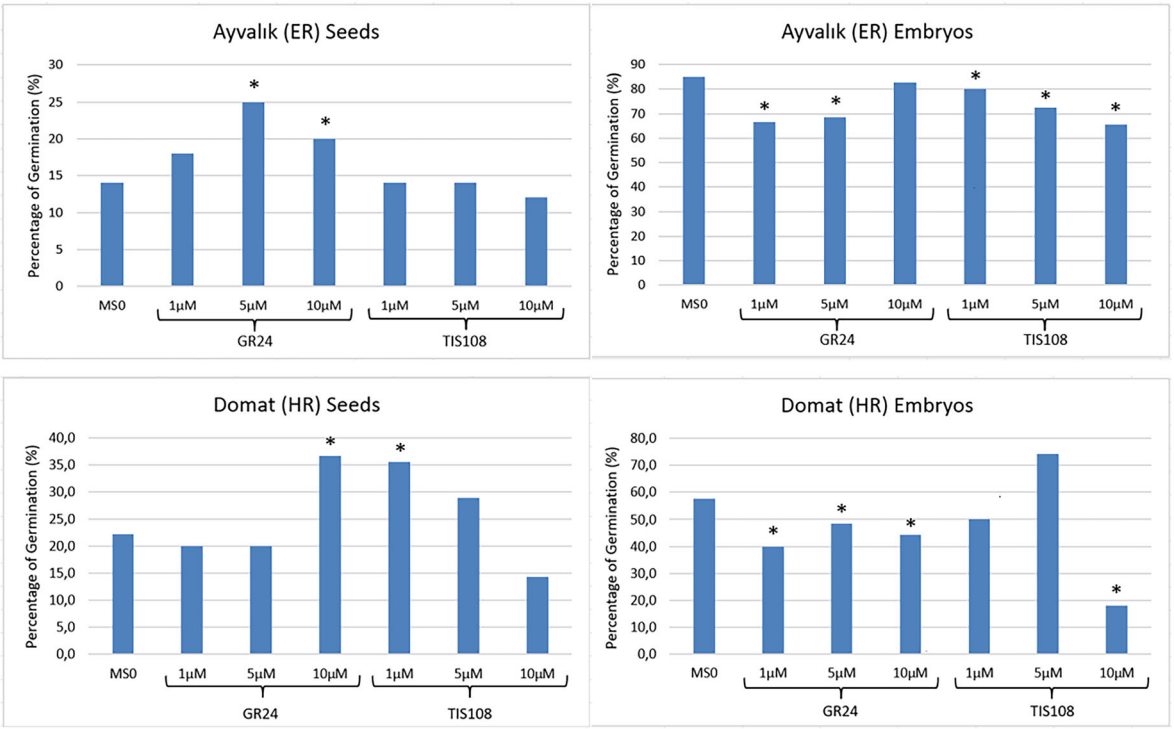

FIGURE 8 Germination percentages of seeds and embryos of easy-to-root (ER) and hard-to-root (HR). The statistical significance is determined by the Kruskal–Wallis test followed by Dunn's post hoc test with Bonferroni correction at $p < .05$ level of significance (*), $n = 35–50$.

applied to the explants. Additionally, we analyzed root lengths, the number of lateral branches, and internode lengths.

The germination frequency of ER seeds treated with *rac*-GR24 was higher compared with the control group (Figure 8). Notably, 5 and 10 µM *rac*-GR24 treatments significantly increased the germination percentage in ER. In contrast, when ER seeds were treated with TIS108, their germination frequency was similar to that of the control group. However, embryos treated with either *rac*-GR24 or TIS108 did not exhibit improved germination compared with the control group for ER (Figure 8). Interestingly, the germination frequency of HR seeds increased significantly when treated with the highest concentration of *rac*-GR24 but decreased with the same concentration of TIS108 (Figure 8). The highest germination rate among the application groups was observed in HR embryos (74%) cultured on MS medium supplemented with 5 µM TIS108, indicating a positive effect of TIS108 on HR embryos, a response not observed in ER embryos.

Root lengths were measured after 4 weeks of culture. For the ER control group, average root lengths were 4.15 ± 1.25 cm for seed-derived seedlings and 3.36 ± .28 cm for embryo-derived seedlings

(Figure 9). When treated with various concentrations of *rac*-GR24 or TIS108, average root lengths for seed-derived seedlings in the ER cultivar ranged from 1.5 to 4.4 cm and 1.5 to 2.7 cm, respectively. For embryo-derived seedlings, the lengths varied between 3.2 and 4.1 cm and 3.3 and 4.3 cm, respectively, for *rac*-GR24 or TIS108. In the HR control group, average root lengths were 3.58 ± 1.12 cm for seed-derived seedlings and 4.82 ± .49 cm for embryo-derived seedlings (Figure 9). The average root lengths for seed-derived HR seedlings varied between 1.4 and 3.7 cm and .8 and 4.6 cm when treated with *rac*-GR24 and TIS108, and for embryo-derived HR seedlings, the lengths ranged from 2.8 to 4.1 cm and 3.9 to 6 cm, respectively. Notably, HR embryos cultured on MS medium supplemented with 5 μM TIS108 exhibited the highest root lengths among all application groups, averaging 6 cm. However, no statistically significant difference was observed between the control and treatment groups for both ER and HR in terms of root lengths. Furthermore, the average root lengths of embryo-derived seedlings were consistently higher than those of seed-derived seedlings for both cultivars.

We also assessed the number of lateral branches and measured the internode lengths in 6-month-old plants derived from both seeds and embryos treated with *rac*-GR24 and TIS108. In the ER cultivar, the average number of lateral branches per individual was .083 and .4 for the control groups of seed-derived and embryo-derived seedlings, respectively (Figure 10). For seed-derived seedlings treated with *rac*-GR24 and TIS108, the range of lateral branch numbers varied from 0 to .4 and .25 to 1, respectively. For embryo-derived seedlings, these numbers ranged from .07 to .4 and .1 to 4, depending on the concentration of PGRs. Notably, in seed-derived seedlings, 1 μM *rac*-GR24 and 1–10 μM TIS108 treatments significantly increased the number of lateral branches, whereas no lateral branches were observed with 5 μM *rac*-GR24 treatment. Additionally, 1 and 5 μM *rac*-GR24 and 1 μM TIS108 treatments significantly reduced the number of lateral branches in embryo-derived ER seedlings. For the HR cultivar, the average number of lateral branches per individual was .75 and 2.56 for the control groups of seed-derived and embryo-derived seedlings, respectively (Figure 10). The lateral branch numbers for seed-derived seedlings treated with *rac*-GR24 and TIS108 varied between 0 and 1.7 and 2 and 3.1, while for embryo-derived seedlings, these numbers ranged from .4 to .7 and .4 to 1.2, respectively. The only treatment group in seed-derived HR seedlings showing a statistically significant increase in lateral branches compared with the control was the one treated with 10 μM TIS108. Conversely, all *rac*-GR24 and TIS108 treatments, except for 1 μM TIS108, significantly decreased the number of lateral branches in embryo-derived HR seedlings.

We subsequently measured the internode lengths of ER and HR seedlings. In the ER control group, the average internode length was 4.09 ± .2 cm for seed-derived seedlings and 5.07 ± .31 cm for embryo-derived seedlings (Figure 11). When treated with various concentrations of *rac*-GR24 or TIS108, the average internode lengths for ER seed-derived seedlings varied between 4.4 and 4.9 cm and 3.9 and 6 cm, respectively, while for embryo-derived seedlings, they ranged from 4.8 to 5.2 cm and 4.8 to 5.8 cm. However, no statistically significant differences were observed between the control and treatment groups of the ER cultivar in terms of internode lengths. In the HR control group, the average internode lengths were 6.05 ± .51 cm for seed-derived seedlings and 5.85 ± .3 cm for embryo-derived seedlings

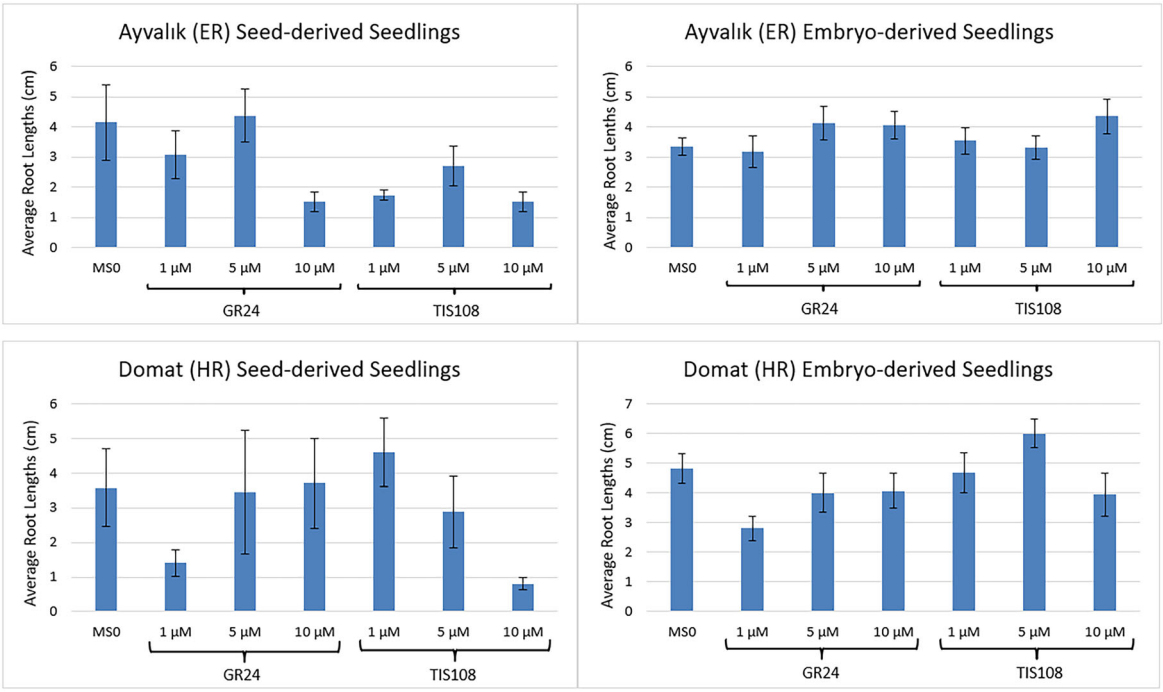

FIGURE 9 Average root lengths of seed and embryo-derived seedlings of easy-to-root (ER) and hard-to-root (HR). The statistical significance is determined by the one-way ANOVA test at $p < .05$ level of significance (*), $n = 5–34$, and error bars represent the standard error of the mean.

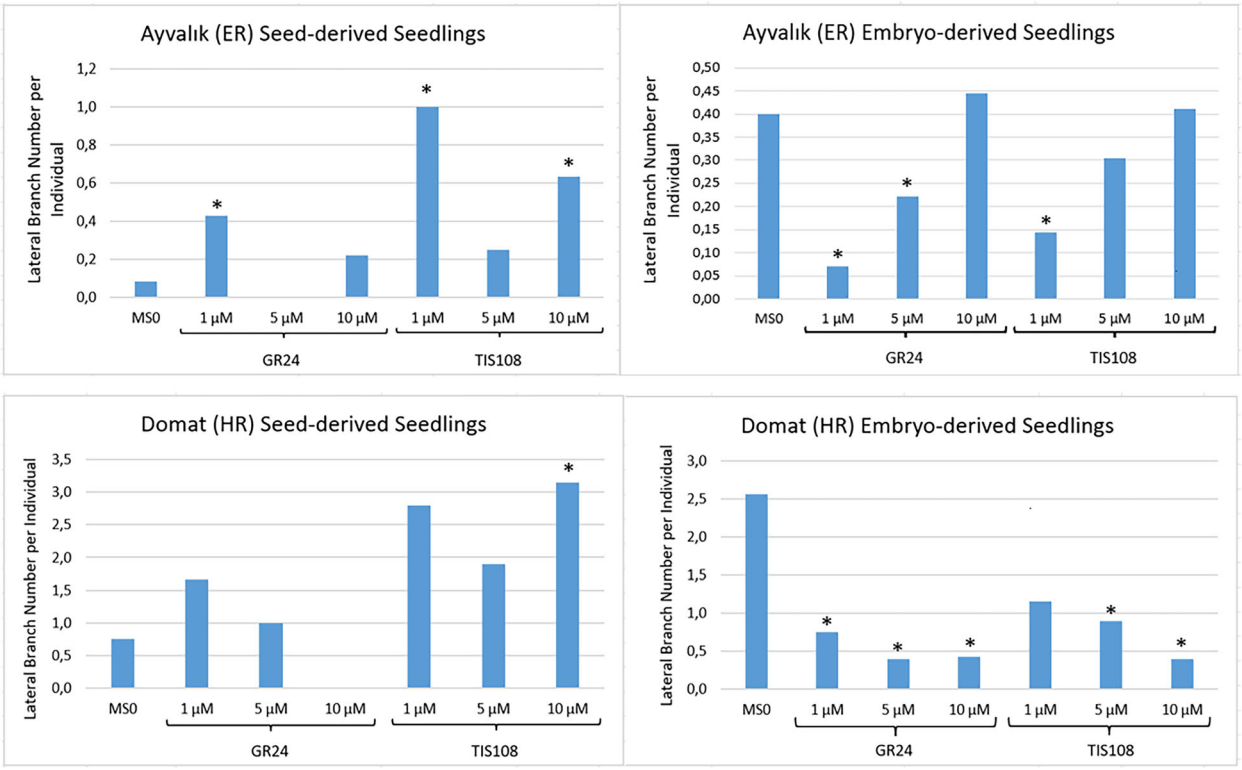

FIGURE 10 Lateral branch number per individual of seed and embryo-derived seedlings of easy-to-root (ER) and hard-to-root (HR). The statistical significance is determined by the Kruskal–Wallis test followed by Dunn's post hoc test with Bonferroni correction at $p < .05$ level of significance (*), $n = 5–23$.

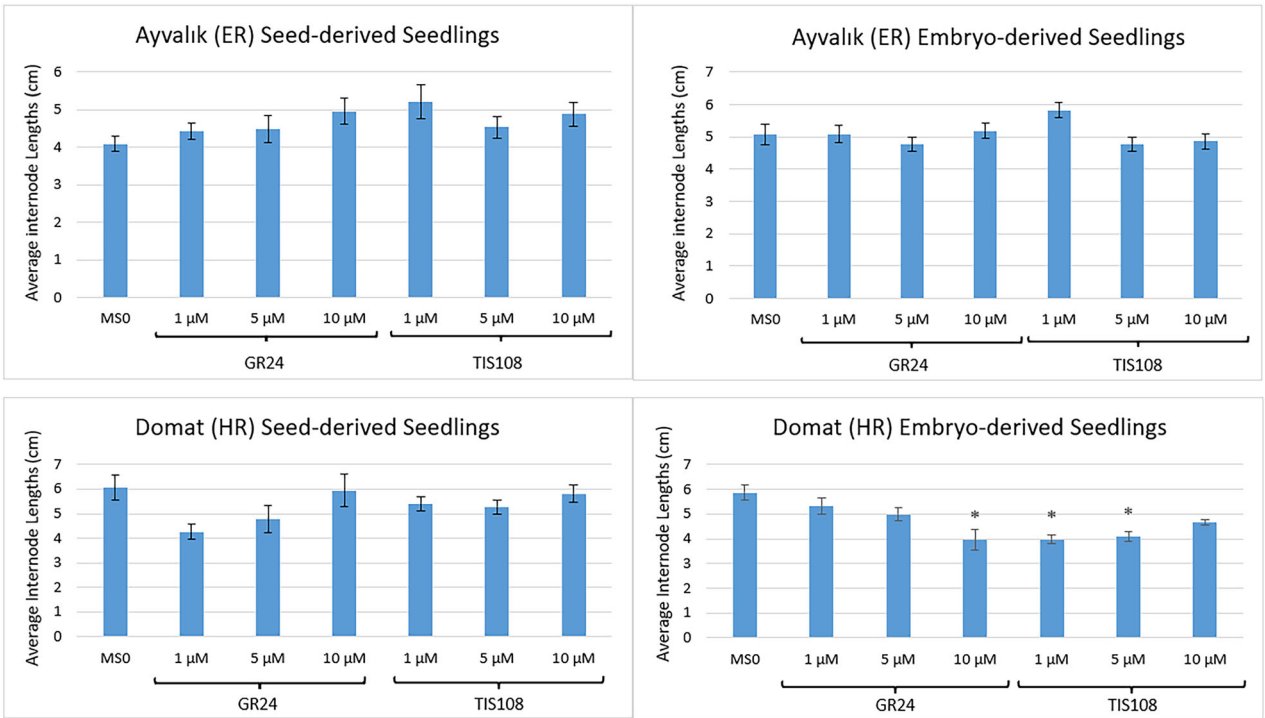

FIGURE 11 Average internode lengths of seed and embryo-derived seedlings of easy-to-root (ER) and hard-to-root (HR). The statistical significance is determined by the one-way ANOVA test at $p < .05$ level of significance (*), $n = 5–23$, and error bars represent the standard error of the mean.

(Figure 11). For HR seedlings treated with *rac*-GR24 and TIS108, the average internode lengths for seed-derived seedlings ranged from 4.3 to 5.9 cm and 5.3 to 5.8 cm, respectively, while for embryo-derived seedlings, they varied between 3.9 and 5.3 cm and 4 and 4.6 cm. Though there were no significant differences for seed-derived seedlings, for embryo-derived HR seedlings, significant differences in internode lengths were observed for the 10 µM *rac*-GR24, 1 µM, and 5 µM TIS108 groups compared with the control group.

The effects of 1, 5, and 10 µM *rac*-GR24 and TIS108 on nodal explants of ER and HR were evaluated after 4 weeks in culture (Figure 3b). Lateral buds were observed in 28.6% of ER and 58.8% of HR explants in total, cultured on OM supplemented with *rac*-GR24 and TIS108. However, the lateral bud formation varied with the concentrations of *rac*-GR24 and TIS108. OM supplemented with 1 µM TIS108 produced the highest number of lateral buds in the HR cultivar (30.8%), while the same concentration for ER resulted in significantly fewer lateral buds (6.3%), suggesting that TIS108 may be effective for the micropropagation of HR olive cultivars in vitro (Figure 12). Zeatin was used as the positive control for statistical analysis because no shoot growth was observed in the ER cultivar on OM0.

4 | DISCUSSION

The bioinformatic analysis of the promoter regions of SL genes in olive revealed the presence of response elements to environmental stress and other hormones. The relationship between light response and SL has been previously explored in various plants including *A. thaliana*, tomato, rice, cucumber, and chrysanthemum (Hu et al., 2010; Koltai et al., 2011; Mashiguchi et al., 2009; Mayzlish-Gati et al., 2010; Thula et al., 2023; Wen et al., 2016; Zhou et al., 2022). Studies have shown that transcript levels of SL genes are influenced by different light conditions (Koltai et al., 2011; Wen et al., 2016), and exogenous SL can regulate light-responsive genes (Mashiguchi et al., 2009; Mayzlish-Gati et al., 2010) as well as plant growth and adaptation (Hu et al., 2010; Thula et al., 2023; Zhou et al., 2022). This suggests that SL promoter elements in olives might play a role in light response. Additionally, previous research has indicated crosstalk between SLs and other hormones in shoot branching (Foo et al., 2005; Ito et al., 2017; Liu et al., 2015; Yi et al., 2023; Yu et al., 2021). For instance, SLs act as positive regulators in disease response in cotton through hormonal crosstalk (Yi et al., 2023). Transcript levels of SL biosynthesis and signaling genes can be modulated by auxin, abscisic acid, or gibberellin (Foo et al., 2005; Ito et al., 2017; Liu et al., 2015), and SLs interact with auxin at the protein level in tomato (Yu et al., 2021). Therefore, the response elements found in olive SL gene promoters might be implicated in this hormonal regulation. Moreover, environmental stresses such as drought, salinity, or heat impact SL biosynthesis and signaling (Ha et al., 2014; Toh et al., 2012). Exogenous SL treatment has been shown to enhance tolerance to abiotic stress (Chen, Xu, et al., 2022; Zhang et al., 2022; Zheng et al., 2021), suggesting that SL promoter motifs in olive might play a role in managing environmental stress. Furthermore, docking results revealed the lowest binding affinity value (−7.0 Kcal/mol) and D-ring interaction of Medicaol (isolated from *Medicago truncatula*, Tokunaga et al., 2014) with OeD14. This suggests that olives might possess species-specific canonical orobanchol-type SL.

The SL biosynthetic and signaling genes have been previously identified in a woody plant poplar (Czarnecki et al., 2014; Zheng et al., 2016), and our study provides additional evidence that the SL biosynthesis pathway is conserved in woody perennials. Transcripts from the "Ayvalık" cultivar showed a 99%–100% match with those of the olive "Sylvestris" cultivar, indicating conservation of SL genes among olive cultivars.

We observed that SL biosynthetic gene expression levels (*D27*, *MAX3*, *MAX4*, and *MAX1*) were high in the root/basal portions of cuttings of both ER and HR olive cultivars, with the exception of *D27* and *MAX1* in HR. Similarly, these genes have been highly expressed in the roots of various plant species such as rice, *A. thaliana*, *M. truncatula*, pea, petunia, tomato, poplar, and chrysanthemum (Booker et al., 2004; Czarnecki et al., 2014; Drummond et al., 2009; Foo et al., 2005; Johnson et al., 2006; Kohlen et al., 2012; Liang et al., 2010; Lin et al., 2009; Liu et al., 2011; Mashiguchi et al., 2009; Snowden et al., 2005; Sorefan et al., 2003; Vogel et al., 2010). Furthermore, the expression levels of SL signaling genes (*D14* and *MAX2*) were notably high in the lateral bud tissues of both ER and HR olive

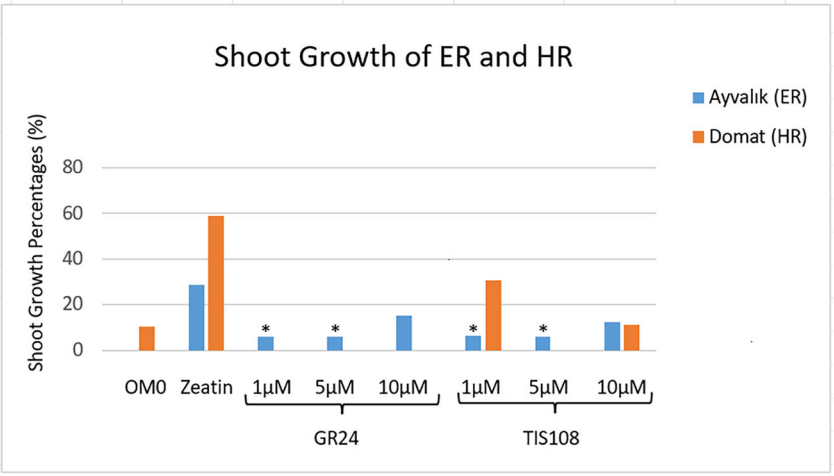

FIGURE 12 Percentages of shoot growth in single node explants of easy-to-root (ER) and hard-to-root (HR). The statistical significance is determined by the Kruskal–Wallis test followed by Dunn's post hoc test with Bonferroni correction at $p < .05$ level of significance (*), $n = 20$. Zeatin is used as a positive control and statistically significant groups were determined by comparison with zeatin.

cultivars. This pattern aligns with findings in other plant species, with *D14* being highly expressed in rice, petunia, and poplar (Arite et al., 2009; Hamiaux et al., 2012; Zheng et al., 2016), and *MAX2* in *A. thaliana*, pea, chrysanthemum, and poplar (Czarnecki et al., 2014; Dong et al., 2013; Johnson et al., 2006; Stirnberg et al., 2007). Our results are consistent with these previous studies, supporting the notion that the higher expression of SL signaling genes in lateral buds may be indicative of the role of SLs in controlling shoot branching in olives.

SL biosynthetic gene expressions were found to be significantly lower in the basal portion of the cuttings in HR cultivars compared with ER roots. However, SL signaling genes showed higher expression in the lateral buds of HR compared with ER. This suggests cultivar-specific differences in SL levels. Previous research has indicated that SLs can inhibit adventitious rooting (Rasmussen et al., 2012). The combination of high signaling gene expression in lateral buds, reduced SL biosynthesis in the basal portion of HR cuttings, and comparatively higher SL biosynthesis in lateral, apical, and leaf tissues suggests that the HR olive cultivar may have higher SL levels than ER. These elevated SL levels in HR could potentially contribute to the inhibition of adventitious rooting in HR woody plants.

In several plant species, including rice (Lin et al., 2009), tomato (Al-Amri et al., 2023; López-Ráez et al., 2008), maize, sorghum, proso millet (Siame et al., 1993), pea (Xie et al., 2009), and *A. thaliana* (Goldwasser et al., 2008), SLs released from roots have been reported to stimulate the germination of parasitic plant seeds. Our results showed an increase in germination frequency when olive seeds were treated with *rac*-GR24, though this effect was not evident in embryos. This suggests that *rac*-GR24 could be beneficial for genotypes with seed germination issues. Conversely, high concentrations of TIS108 reduced the germination frequency of both seeds and embryos. While TIS108 has been previously noted to promote the germination of parasitic plant seeds (Bao et al., 2017), it significantly decreased olive seed germination in our study compared with the control group.

The impact of *rac*-GR24 on main root length has been documented in model plants, where SL analog GR24 application increased primary or seminal root length in *A. thaliana* and rice (Richmond et al., 2022; Ruyter-Spira et al., 2011; Sun et al., 2014). For instance, *A. thaliana* plants treated with 1.25 and 2.5 μM GR24 exhibited extended main root lengths, whereas higher concentrations (5 and 10 μM GR24) resulted in shorter roots (Ruyter-Spira et al., 2011). Consistent with this, according to our results, root lengths in ER seed-derived seedlings decreased when treated with 10 μM *rac*-GR24 compared with the control group. Additionally, the TIS108 application similarly reduced root lengths, echoing observations in SL biosynthetic mutants (Drummond et al., 2009; Guan et al., 2012). Variations in responses to *rac*-GR24 and TIS108 treatments across different cultivars and explant types suggest that the effects of SL on main root length are likely species-specific or dependent on growth conditions.

Previous studies have demonstrated that SL mutants exhibit increased branching compared with wild-type plants across many species (Chen, Wang, et al., 2023; Gomez-Roldan et al., 2008; Guan et al., 2012; Hamiaux et al., 2012; Umehara et al., 2008). In our study, lateral branch numbers per individual were significantly inhibited by *rac*-GR24 in embryo-derived seedlings, and in some concentrations, completely suppressed in groups of seed-derived seedlings. Conversely, TIS108 applications significantly increased branching in seed-derived seedlings. A similar increase in branching was observed in *A. thaliana* treated with 1 and 3 μM TIS108 (Ito et al., 2013). These findings suggest that both SLs and their inhibitors can potentially modulate branching patterns in olives. However, for HR seedlings derived from embryos, both *rac*-GR24 and TIS108 inhibited branching, indicating the importance of genotype.

In the ER cultivar, internode lengths were consistent across all treatment and control groups. This is in line with a study on rice where 1 μM GR24 application did not significantly alter plant height (Nakamura et al., 2013), however, the plant height increased as a result of the 2 μM GR24 application (Umehara et al., 2008). Additionally, in pea, a 3 μM GR24 application did not significantly affect internode length (de Saint Germain et al., 2013). For HR, only embryo-derived seedlings treated with 10 μM *rac*-GR24, 1 μM, and 5 μM TIS108 exhibited statistically significant shorter internode lengths than the control group. Although the reduction in internode length with 10 μM *rac*-GR24 was unexpected, similar outcomes with TIS108 are consistent with observations in SL biosynthesis or signaling mutants of other species, such as petunia (Snowden et al., 2005), pea (de Saint Germain et al., 2013), rice (Du et al., 2023; Lin et al., 2009), maize (Guan et al., 2012), and tomato (Lu et al., 2023), where internode distances or plant heights decreased compared with wild-type plants.

For the applications of *rac*-GR24 and TIS108 on nodal explants, the most effective results were observed with OM0 medium supplemented with 1 μM TIS108 in HR explants, achieving a 30.8% success rate. While the shoot growth rates were lower compared with those with zeatin applications, these findings demonstrate the potential of TIS108 to induce lateral bud growth in the HR cultivar. This suggests that SL inhibitors could be useful for propagating other HR olive cultivars. However, the same effect was not observed in the ER cultivar, indicating a cultivar-specific response mechanism. Similarly, recent reports have highlighted the positive impact of TIS108 on shoot regeneration in woody plants (Asghar et al., 2022).

In conclusion, the molecular characterization of SL genes in olives is of critical importance, especially considering the long periods typically required for conventional breeding in woody plants. Our study reveals that SLs can significantly influence lateral branching in olives. Both ER and HR seed-derived seedlings exhibited increased branching when treated with TIS108. These insights contribute valuable knowledge towards the understanding of SLs in plant development and offer potential strategies for olive cultivation and breeding.

AUTHOR CONTRIBUTIONS

Aslıhan Özbilen and Kemal Melih Taşkin designed the research, Aslıhan Özbilen and Kemal Melih Taşkin performed the research, Aslıhan Özbilen and Fatih Sezer analyzed data, Aslıhan Özbilen wrote, and Kemal Melih Taşkin supervised the paper.

ACKNOWLEDGMENTS

This study is partially based on a Ph.D. thesis entitled "Characterization of the Genes Involved in Strigolactone Biosynthesis in Olive (*Olea europaea* L.)" from Çanakkale Onsekiz Mart University, supported by The Scientific and Technological Research Council of Turkey (TUBITAK) with a project number 215O543 and COST Action (FA1206). We thank TUBITAK for their support and the doctoral scholarship (2211-A program). We also thank the Edremit Directorate of Olive Production Station (Edremit, Balıkesir) for providing the biological material.

CONFLICT OF INTEREST STATEMENT

The authors declare no conflict of interest.

PEER REVIEW

The peer review history for this article is available in the Supporting Information for this article.

DATA AVAILABILITY STATEMENT

All data are presented in this manuscript.

ORCID

Aslıhan Özbilen https://orcid.org/0000-0002-2034-4682
Fatih Sezer https://orcid.org/0000-0002-9436-0191
Kemal Melih Taşkin https://orcid.org/0000-0002-3746-0508

REFERENCES

Abe, S., Sado, A., Tanaka, K., Kisugi, T., Asami, K., Ota, S., Kim, H. I., Yoneyama, K., Xie, X., Ohnishi, T., Seto, Y., Yamaguchi, S., Akiyama, K., Yoneyama, K., & Nomura, T. (2014). Carlactone is converted to carlactonoic acid by MAX1 in Arabidopsis and its methyl ester can directly interact with AtD14 in vitro. *Proceedings of the National Academy of Sciences*, *111*(50), 18084–18089. https://doi.org/10.1073/pnas.1410801111

Agusti, J., Herold, S., Schwarz, M., Sanchez, P., Ljung, K., Dun, E. A., Brewer, P. B., Beveridge, C. A., Sieberer, T., Sehr, E. M., & Greb, T. (2011). Strigolactone signaling is required for auxin-dependent stimulation of secondary growth in plants. *Proceedings of the National Academy of Sciences*, *108*(50), 20242–20247. https://doi.org/10.1073/pnas.1111902108

Akiyama, K., Matsuzaki, K., & Hayashi, H. (2005). Plant sesquiterpenes induce hyphal branching in arbuscular mycorrhizal fungi. *Nature*, *435*(9), 824–827. https://doi.org/10.1038/nature03608

Al-Amri, A. A., Alsubaie, Q. D., Alamri, S. A., & Siddiqui, M. H. (2023). Strigolactone analog GR24 induces seed germination and improves growth performance of different genotypes of tomato. *Journal of Plant Growth Regulation*, *42*, 1–14. https://doi.org/10.1007/s00344-023-10947-8

Al-Babili, S., & Bouwmeester, H. J. (2015). Strigolactones, a novel carotenoid-derived plant hormone. *Annual Review of Plant Biology*, *66*, 161–186. https://doi.org/10.1146/annurev-arplant-043014-114759

Alder, A., Jamil, M., Marzorati, M., Bruno, M., Vermathen, M., Bigler, P., Ghisla, S., Bouwmeester, H., Beyer, P., & Al-babili, S. (2012). The path from b-carotene to carlactone, a strigolactone-like plant hormone. *Science*, *335*, 1348–1350. https://doi.org/10.1126/science.1218094

Almagro Armenteros, J. J., Sønderby, C. K., Sønderby, S. K., Nielsen, H., & Winther, O. (2017). DeepLoc: Prediction of protein subcellular localization using deep learning. *Bioinformatics*, *33*(21), 3387–3395. https://doi.org/10.1093/bioinformatics/btx431

Arite, T., Umehara, M., Ishikawa, S., Hanada, A., Maekawa, M., Yamaguchi, S., & Kyozuka, J. (2009). D14, a strigolactone-insensitive mutant of rice, shows an accelerated outgrowth of tillers. *Plant & Cell Physiology*, *50*(8), 1416–1424. https://doi.org/10.1093/pcp/pcp091

Asghar, S., Xiong, Y., Che, M., Fan, X., Li, H., Wang, Y., Xu, X., Li, W., & Han, Z. (2022). Transcriptome analysis reveals the effects of strigolactone on shoot regeneration of apple. *Plant Cell Reports*, *41*(7), 1613–1626. https://doi.org/10.1007/s00299-022-02882-x

Ballus, C. A., Meinhart, A. D., de Souza Campos, F. A., da Silva, L. F. D. O., de Oliveira, A. F., & Godoy, H. T. (2014). A quantitative study on the phenolic compound, tocopherol, and fatty acid contents of monovarietal virgin olive oils produced in the southeast region of Brazil. *Food Research International*, *62*, 74–83. https://doi.org/10.1016/j.foodres.2014.02.040

Bao, Y. Z., Yao, Z. Q., Cao, X. L., Peng, J. F., Xu, Y., Chen, M. X., & Zhao, S. F. (2017). Transcriptome analysis of *Phelipanche aegyptiaca* seed germination mechanisms stimulated by fluridone, TIS108, and GR24. *PLoS ONE*, *12*(11), e0187539. https://doi.org/10.1371/journal.pone.0187539

Booker, J., Auldridge, M., Wills, S., McCarty, D., Klee, H., & Leysser, O. (2004). MAX3/CCD7 is a carotenoid cleavage dioxygenase required for the synthesis of a novel plant signaling molecule. *Current Biology*, *14*, 1232–1238. https://doi.org/10.1016/j.cub.2004.06.061

Booker, J., Sleberer, T., Wright, W., Williamson, L., Willett, B., Stirnberg, P., Turnbull, C., Srinivasan, M., Goddard, P., & Leyser, O. (2005). MAX1 encodes a cytochrome P450 family member that acts downstream of MAX3/4 to produce a carotenoid-derived branch-inhibiting hormone. *Developmental Cell*, *8*(3), 443–449. https://doi.org/10.1016/j.devcel.2005.01.009

Brewer, P. B., Yoneyama, K., Filardo, F., Meyers, E., Scaffidi, A., Frickey, T., Akiyama, K., Seto, Y., Dun, E. A., Cremer, J. E., Kerr, S. C., Waters, M. T., Flematti, G. R., Mason, M. G., Weiller, G., Yamaguchi, S., Nomura, T., Smith, S. M., Yoneyama, K., & Beveridge, C. A. (2016). *LATERAL BRANCHING OXIDOREDUCTASE* acts in the final stages of strigolactone biosynthesis in *Arabidopsis*. *Proceedings of the National Academy of Sciences*, *113*(22), 6301–6306. https://doi.org/10.1073/pnas.1601729113

Çetintaş Gerakkakis, A., & Özkaya, M. T. (2005). Effects of cutting size, rooting media and planting time on rooting of Domat and Ayvalik olive (*Olea europaea* L.) cultivars in shaded polyethylene tunnel (Spt). *Tarım Bilimleri Dergisi*, *11*(3), 334–338. https://doi.org/10.1501/Tarimbil_0000000581

Chen, C., Xu, L., Zhang, X., Wang, H., Nisa, Z. U., Jin, X., Yu, L., Jing, L., & Chen, C. (2022). Exogenous strigolactones enhance tolerance in soybean seedlings in response to alkaline stress. *Physiologia Plantarum*, *174*(5), e13784. https://doi.org/10.1111/ppl.13784

Chen, G. T. E., Wang, J. Y., Jamil, M., Braguy, J., & Al-Babili, S. (2022). 9-cis-β-Apo-10′-carotenal is the precursor of strigolactones in planta. *Planta*, *256*(5), 88. https://doi.org/10.1007/s00425-022-03999-9

Chen, G. T. E., Wang, J. Y., Votta, C., Braguy, J., Jamil, M., Kirschner, G. K., Fiorilli, V., Berqdar, L., Balakrishna, A., Blilou, I., Lanfranco, L., & al-Babili, S. (2023). Disruption of the rice *4-DEOXYOROBANCHOL HYDROXYLASE* unravels specific functions of canonical strigolactones. *Proceedings of the National Academy of Sciences*, *120*(42), e2306263120. https://doi.org/10.1073/pnas.2306263120

Chen, S., Song, X., Zheng, Q., Liu, Y., Yu, J., Zhou, Y., & Xia, X. (2023). The transcription factor SPL13 mediates strigolactone suppression of shoot branching by inhibiting cytokinin synthesis in *Solanum lycopersicum*. *Journal of Experimental Botany*, *74*(18), 5722–5735.

Cook, C. E., Whichard, L. P., Turner, B., Wall, M. E., & Egley, G. H. (1966). Germination of witchweed (*Striga lutea* Lour.): Isolation and

properties of a potent stimulant. *Science*, *154*, 1189–1190. https://doi.org/10.1126/science.154.3753.1189

Cui, J., Nishide, N., Mashiguchi, K., Kuroha, K., Miya, M., Sugimoto, K., & Izawa, T. (2023). Fertilization controls tiller numbers via transcriptional regulation of a MAX1-like gene in rice cultivation. *Nature Communications*, *14*(1), 3191. https://doi.org/10.1038/s41467-023-38670-8

Czarnecki, O., Yang, J., Wang, X., Wang, S., Muchero, W., Tuskan, G. A., & Chen, J. (2014). Characterization of *MORE AXILLARY GROWTH* genes in *Populus*. *PLoS ONE*, *9*(7), e102757. https://doi.org/10.1371/journal.pone.0102757

Czarnecki, O., Yang, J., Weston, D. J., Tuskan, G. A., & Chen, J. G. (2013). A dual role of strigolactones in phosphate acquisition and utilization in plants. *International Journal of Molecular Sciences*, *14*(4), 7681–7701. https://doi.org/10.3390/ijms14047681

de Saint Germain, A., Ligerot, Y., Dun, E. A., Pillot, J., Ross, J. J., Beveridge, C. A., & Rameau, C. (2013). Strigolactones stimulate internode elongation independently of gibberellins. *Plant Physiology*, *163*, 1012–1025. https://doi.org/10.1104/pp.113.220541

Dong, L., Ishak, A., Yu, J., Zhao, R., & Zhao, L. (2013). Identification and functional analysis of three MAX2 orthologs in chrysanthemum. *Journal of Integrative Plant Biology*, *55*(5), 434–442. https://doi.org/10.1111/jipb.12028

Drummond, R. S. M., Martinez-Sanchez, M., Janssen, B. J., Templeton, K. R., Simons, J. L., Quinn, B. D., Karunairetnam, S., & Snowden, K. C. (2009). *Petunia hybrida CAROTENOID CLEAVAGE DIOXYGENASE7* is involved in the production of negative and positive branching signals in petunia. *Plant Physiology*, *151*, 1867–1877. https://doi.org/10.1104/pp.109.146720

Du, L., Yan, J., Yu, C., Wang, C., Tan, W., & Duan, L. (2023). Design, synthesis and biological evaluation of novel 1 H-1, 2, 4-triazole derivatives as strigolactone biosynthesis inhibitors. *Journal of Plant Growth Regulation*, 1–14. https://doi.org/10.1007/s00344-023-11133-6

Edgar, R. C. (2004). MUSCLE: Multiple sequence alignment with high accuracy and high throughput. *Nucleic Acids Research*, *32*(5), 1792–1797. https://doi.org/10.1093/nar/gkh340

Fabbri, A., Bartolini, G., Lambardi, M., & Kailis, S. (2004). *Olive propagation manual* (p. 158). CSIRO.

Fabbri, A., Lambardi, M., & Ozden-Tokatli, Y. (2009). Olive breeding. In *Breeding plantation tree crops: Tropical species* (pp. 423–465). Springer. https://doi.org/10.1007/978-0-387-71201-7_12

Fiorilli, V., Wang, J. Y., Bonfante, P., Lanfranco, L., & Al-Babili, S. (2019). Apocarotenoids: Old and new mediators of the arbuscular mycorrhizal symbiosis. *Frontiers in Plant Science*, *10*, 1186. https://doi.org/10.3389/fpls.2019.01186

Foo, E., Bullier, E., Goussot, M., Foucher, F., Rameau, C., & Beveridge, C. A. (2005). The branching gene RAMOSUS1 mediates interactions among two novel signals and auxin in pea. *The Plant Cell.*, *17*, 464–474. https://doi.org/10.1105/tpc.104.026716

Garcia, J. L., Troncoso, J., Sarmiento, R., & Troncoso, A. (2002). Influence of carbon source and concentration on the in vitro development of olive zygotic embryos and explants raised from them. *Plant Cell Tissue and Organ*, *69*, 95–100. https://doi.org/10.1023/A:1015086104389

Gasteiger, E., Hoogland, C., Gattiker, A., Duvaud, S., Wilkins, M. R., Appel, R. D., & Bairoch, A. (2005). Protein identification and analysis tools on the ExPASy server. In *The proteomics protocols handbook* (pp. 571–607). Humana Press.

Goldwasser, Y., Yoneyama, K., Xie, X., & Yoneyama, K. (2008). Production of Strigolactones by *Arabidopsis thaliana* responsible for *Orobanche aegyptiaca* seed germination. *Plant Growth Regulation*, *55*, 21–28. https://doi.org/10.1007/s10725-008-9253-z

Gomez-Roldan, V., Fermas, S., Brewer, P. B., Puech-Pages, V., Dun, E. A., Pillot, J., Letisse, F., Matusova, R., Danoun, S., Portais, J., Bouwmeester, H., Becard, G., Beveridge, C. A., Rameau, C., & Rochange, S. F. (2008). Strigolactone inhibition of shoot branching. *Nature*, *455*(11), 189–194. https://doi.org/10.1038/nature07271

Guan, J. C., Koch, K. E., Suzuki, M., Wu, S., Latshaw, S., Petruff, T., Goulet, C., Klee, H. J., & McCarty, D. R. (2012). Diverse roles of strigolactone signaling in maize architecture and the uncoupling of a branching-specific subnetwork. *Plant Physiology*, *160*, 1303–1317. https://doi.org/10.1104/pp.112.204503

Ha, C. V., Leyva-González, M. A., Osakabe, Y., Tran, U. T., Nishiyama, R., Watanabe, Y., Tanaka, M., Seki, M., Yamaguchi, S., Dong, N. V., Yamaguchi-Shinozaki, K., Shinozaki, K., Herrera-Estrella, L., & Tran, L. S. P. (2014). Positive regulatory role of strigolactone in plant responses to drought and salt stress. *PNAS Nexus*, *111*, 851–856. https://doi.org/10.1073/pnas.1322135111

Hamiaux, C., Drummond, R. S. M., Janssen, B. J., Ledger, S. E., Cooney, J. M., Newcomb, R. D., & Snowden, K. C. (2012). DAD2 is an α/β hydrolase likely to be involved in the perception of the plant branching hormone, strigolactone. *Current Biology*, *22*, 2032–2036. https://doi.org/10.1016/j.cub.2012.08.007

Hu, Z., Yan, H., Yang, J., Yamaguchi, S., Maekawa, M., Takamure, I., Tsutsumi, N., Kyozuka, J., & Nakazono, M. (2010). Strigolactones negatively regulate mesocotyl elongation in rice during germination and growth in darkness. *Plant & Cell Physiology*, *51*(7), 1136–1142. https://doi.org/10.1093/pcp/pcq075

Hürkan, K., Sezer, F., Özbilen, A., & Taşkın, K. M. (2018). Identification of reference genes for real-time quantitative polymerase chain reaction based gene expression studies on various olive (*Olea europaea* L.) tissues. *The Journal of Horticultural Science and Biotechnology*, *93*(6), 644–651. https://doi.org/10.1080/14620316.2018.1427005

Ito, S., Braguy, J., Wang, J. Y., Yoda, A., Fiorilli, V., Takahashi, I., Jamil, M., Felemban, A., Miyazaki, S., Mazzarella, T., Chen, G. E., Shinozawa, A., Balakrishna, A., Berqdar, L., Rajan, C., Ali, S., Haider, I., Sasaki, Y., Yajima, S., … al-Babili, S. (2022). Canonical strigolactones are not the major determinant of tillering but important rhizospheric signals in rice. *Science Advances*, *8*(44), eadd1278. https://doi.org/10.1126/sciadv.add1278

Ito, S., Umehara, M., Hanada, A., Yamaguchi, S., & Asami, T. (2013). Effects of strigolactone-biosynthesis inhibitör TIS108 on *Arabidopsis*. *Plant Signalling and Behaviour.*, *8*(5), e24193. https://doi.org/10.4161/psb.24193

Ito, S., Yamagami, D., Umehara, M., Hanada, A., Yoshida, S., Sasaki, Y., Yajima, S., Kyozuka, J., Ueguchi-Tanaka, M., Matsuoka, M., Shirasu, K., Yamaguchi, S., & Asami, T. (2017). Regulation of strigolactone biosynthesis by gibberellin signaling. *Plant Physiology*, *174*, 1250–1259. https://doi.org/10.1104/pp.17.00301

Jiang, L., Liu, X., Xiong, G., Liu, H., Chen, F., Wang, L., Meng, X., Liu, G., Yu, H., Yuan, Y., Yi, W., Zhao, L., Ma, H., He, Y., Wu, Z., Melcher, K., Qian, Q., Xu, H. E., Wang, Y., & Li, J. (2013). DWARF 53 acts as a repressor of strigolactone signalling in rice. *Nature*, *1-5*, 401–405. https://doi.org/10.1038/nature12870

Johnson, X., Brcich, T., Dun, E. A., Goussot, M., Haurogne, K., Beveridge, C. A., & Rameau, C. (2006). Branching genes are conserved across species. Genes controlling a novel signal in pea are coregulated by other long-distance signals. *Plant Physiology*, *142*, 1014–1026. https://doi.org/10.1104/pp.106.087676

Kagiyama, M., Hirano, Y., Mori, T., Kim, S. Y., Kyozuka, J., Seto, Y., Yamaguchi, S., & Hakoshima, T. (2013). Structures of D 14 and D 14 L in the strigolactone and karrikin signaling pathways. *Genes to Cells*, *18*(2), 147–160. https://doi.org/10.1111/gtc.12025

Kearse, M., Moir, R., Wilson, A., Stones-Havas, S., Cheung, M., Sturrock, S., Buxton, S., Cooper, A., Markowitz, C. D., Duran, C., Thierer, T., Ashton, B., Meintjes, P., & Drummond, A. (2012). Geneious basic: An integrated and extendable desktop software platform for the

organization and analysis of sequence data. *Bioinformatics*, *28*(12), 1647–1649. https://doi.org/10.1093/bioinformatics/bts199

Kohlen, W., Charnikhova, T., Lammers, M., Pollina, T., Toth, P., Haider, I., Pozo, M. J., de Maagd, R. A., Ruyter-Spira, C., Bouwmeester, H. J., & Lopez-Raez, J. A. (2012). The tomato *CAROTENOID CLEAVAGE DIOXYGENASE8* (*SlCCD8*) regulates rhizosphere signaling, plant architecture and affects reproductive development through strigolactone biosynthesis. *The New Phytologist*, *196*, 535–547. https://doi.org/10.1111/j.1469-8137.2012.04265.x

Koltai, H., Cohen, M., Chesin, O., Mayzlish-Gati, E., Becard, G., Puech, V., Dor, B. B., Resnick, N., Wininger, S., & Kapulnik, Y. (2011). Light is a positive regulator of strigolactone levels in tomato roots. *Journal of Plant Physiology*, *168*(1), 1993–1996. https://doi.org/10.1016/j.jplph.2011.05.022

Lescot, M., Dehais, P., Thijs, G., Marchal, K., Moreau, Y., Van der Peer, Y., Rouze, P., & Rombauts, S. (2002). PlantCARE, a database of plant cis-acting regulatory elements and a portal to tools for in silico analysis of promoter sequences. *Nucleic Acids Research*, *30*(1), 325–327. https://doi.org/10.1093/nar/30.1.325

Leva, A. R., Petruccelli, R., & Bartolini, G. (1994). Mannitol "in vitro" culture of *Olea europaea* L. (cv. Maurino). *Acta Horticulturae*, *356*, 43–46. https://doi.org/10.17660/ActaHortic.1994.356.7

Liang, J., Zhao, L., Challis, R., & Leyser, O. (2010). Strigolactone regulation of shoot branching in chrysanthemum (*Dendranthema grandiflorum*). *Journal of Experimental Botany*, *61*(11), 3069–3078. https://doi.org/10.1093/jxb/erq133

Lin, H., Wang, R., Qian, Q., Yan, M., Meng, X., Fu, Z., Yan, C., Jiang, B., Su, Z., Li, J., & Wang, Y. (2009). DWARF27, an iron-containing protein required for the biosynthesis of strigolactones, regulates rice tiller bud outgrowth. *The Plant Cell.*, *21*, 1512–1525. https://doi.org/10.1105/tpc.109.065987

Liu, J., He, H., Vitali, M., Visentin, I., Charnikhova, T., Haider, I., Schubert, A., Ruyter-Spira, C., Bouwmeester, H. J., Lovisolo, C., & Cardinale, F. (2015). Osmotic stress represses strigolactone biosynthesis in *Lotus japonicus* roots: Exploring the interaction between strigolactones and ABA under abiotic stress. *Planta*, *241*, 1435–1451. https://doi.org/10.1007/s00425-015-2266-8

Liu, W., Kohlen, W., Lillo, A., op den Camp, R., Ivanov, S., Hartog, M., Limpens, E., Jamil, M., Smaczniak, C., Kaufmann, K., Yang, W. C., Hooiveld, G. J. E. J., Charnikhova, T., Bouwmeester, H. J., Bisseling, T., & Geurts, R. (2011). Strigolactone biosynthesis in *Medicago truncatula* and rice requires the symbiotic GRAS-type transcription factors NSP1 and NSP2. *The Plant Cell*, *23*(10), 3853–3865. https://doi.org/10.1105/tpc.111.089771

López-Ráez, J. A., Charnikhova, T., Gomez-Roldan, V., Matusova, R., Kohlen, W., de Vos, R., Verstappen, F., Puech-Pages, V., Becard, G., Mulder, P., & Bouwmeester, H. (2008). Tomato strigolactones are derived from carotenoids and their biosynthesis is promoted by phosphate starvation. *The New Phytologist*, *178*(4), 863–874. https://doi.org/10.1111/j.1469-8137.2008.02406.x

Lu, X., Liu, X., Xu, J., Liu, Y., Chi, Y., Yu, W., & Li, C. (2023). Strigolactone-mediated trehalose enhances salt resistance in tomato seedlings. *Horticulturae*, *9*(7), 770. https://doi.org/10.3390/horticulturae9070770

Lüthy, R., Bowie, J. U., & Eisenberg, D. (1992). Assessment of protein models with three-dimensional profiles. *Nature*, *356*, 83–85. https://doi.org/10.1038/356083a0

Mashiguchi, K., Sasaki, E., Shimada, Y., Nagae, M., Ueno, K., Nakano, T., Yoneyama, K., Suzuki, Y., & Asami, T. (2009). Feedback-regulation of strigolactone biosynthetic genes and strigolactone-regulated genes in Arabidopsis. *Bioscience Biotechnology and Biochemistry*, *73*(11), 2460–2465. https://doi.org/10.1271/bbb.90443

Mayzlish-Gati, E., Lekkala, S. P., Resnick, N., Wininger, S., Bhattacharya, C., Lemcoff, J. H., Kapulnik, Y., & Koltai, H. (2010). Strigolactones are positive regulators of light-harvesting genes in tomato. *Journal of Experimental Botany*, *61*(11), 3129–3136. https://doi.org/10.1093/jxb/erq138

Mitchell, A. L., Attwood, T. K., Babbitt, P. C., Blum, M., Bork, P., Bridge, A., Brown, S. D., Chang, H., el-Gebali, S., Fraser, M. I., Gough, J., Haft, D. R., Huang, H., Letunic, I., Lopez, R., Luciani, A., Madeira, F., Marchler-Bauer, A., Mi, H., … Finn, R. D. (2019). InterPro in 2019: Improving coverage, classification and access to protein sequence annotations. *Nucleic Acids Research*, *47*, 351–360. https://doi.org/10.1093/nar/gky1100

Murashige, T., & Skoog, F. (1962). A revised medium for rapid growth and bio assays with tobacco tissue cultures. *Physiologia Plantarum*, *15*, 473–497. https://doi.org/10.1111/j.1399-3054.1962.tb08052.x

Nakamura, H., Xue, Y., Miyakawa, T., Hou, F., Qin, H., Fukui, K., Shi, X., Ito, E., Ito, S., Park, S., Miyauchi, Y., Asano, A., Totsuka, N., Ueda, T., Tanokura, M., & Asami, T. (2013). Molecular mechanism of strigolactone perception by DWARF14. *Nature Communications*, *4*, 1–10. https://doi.org/10.1038/ncomms3613

Pfaffl, M. W. (2001). A new mathematical model for relative quantification in real-time RT–PCR. *Nucleic Acids Research*, *29*(9), e45. https://doi.org/10.1093/nar/29.9.e45

Pfaffl, M. W. (2004). In S. A. Bustin (Ed.), *Quantification strategies in real time PCR* (pp. 87–112). La Jolla, CA, USA: International University Line.

Porfirio, S., Calado, M. L., Noceda, C., Cabrita, M. J., da Silva, M. G., Azadi, P., & Peixe, A. (2016). Tracking biochemical changes during adventitious root formation in olive (*Olea europaea* L.). *Scientia Horticulturae*, *204*, 41–53. https://doi.org/10.1016/j.scienta.2016.03.029

Rao, G., Zhang, J., Liu, X., Lin, C., Xin, H., Xue, L., & Wang, C. (2021). De novo assembly of a new *Olea europaea* genome accession using nanopore sequencing. *Horticulture Research*, *8*(64), 64. https://doi.org/10.1038/s41438-021-00498-y

Rasmussen, A., Mason, M. G., De Cuyper, C., Brewer, P. B., Herold, S., Agusti, J., Geelen, D., Greb, T., Goormachtig, S., Beeckman, T., & Beveridge, C. A. (2012). Strigolactones suppress adventitious rooting in Arabidopsis and pea. *Plant Physiology*, *158*(4), 1976–1987. https://doi.org/10.1104/pp.111.187104

Richmond, B. L., Coelho, C. L., Wilkinson, H., McKenna, J., Ratchinski, P., Schwarze, M., Frost, M., Lagunas, B., & Gifford, M. L. (2022). Elucidating connections between the strigolactone biosynthesis pathway, flavonoid production and root system architecture in *Arabidopsis thaliana*. *Physiologia Plantarum*, *174*(2), e13681. https://doi.org/10.1111/ppl.13681

Rugini, E. (1986). Olive (Olea europeae L.). In Y. P. S. Bajaj (Ed.), *Biotechnology in agriculture and forestry* (pp. 253–267). Springer.

Ruyter-Spira, C., Kohlen, W., Charnikhova, T., van Zeijl, A., van Bezouwen, L., de Ruijter, N., Cardoso, C., Lopez-Raez, J. A., Matusova, R., Bours, R., Verstappen, F., & Bouwmeester, H. (2011). Physiological effects of the synthetic strigolactone analog GR24 on root system architecture in Arabidopsis: Another belowground role for strigolactones? *Plant Physiology*, *155*, 721–734. https://doi.org/10.1104/pp.110.166645

Schwartz, S. H., Qin, X., & Loewen, M. C. (2004). The biochemical characterization of two carotenoid cleavage enzymes from Arabidopsis indicates that a carotenoid-derived compound inhibits lateral branching. *The Journal of Biological Chemistry*, *279*(45), 46940–46945. https://doi.org/10.1074/jbc.M409004200

Scoditti, E., Capurso, C., Capurso, A., & Massaro, M. (2014). Vascular effects of the Mediterranean diet—Part II: Role of omega-3 fatty acids and olive oil polyphenols. *Vascular Pharmacology*, *63*, 127–134. https://doi.org/10.1016/j.vph.2014.07.001

Scotto-Lavino, E., Du, G., & Frohman, M. A. (2006a). 3′ end cDNA amplification using classic RACE. *Nature Protocols*, *1*(6), 2742–2745. https://doi.org/10.1038/nprot.2006.481

Scotto-Lavino, E., Du, G., & Frohman, M. A. (2006b). 5′ end cDNA amplification using classic RACE. *Nature Protocols*, *1*(6), 2555–2562. https://doi.org/10.1038/nprot.2006.480

Seto, Y., Sado, A., Asami, K., Hanada, A., Umehara, M., Akiyama, K., & Yamaguchi, S. (2014). Carlactone is an endogenous biosynthetic precursor for strigolactones. *Proceedings of the National Academy of Sciences*, *111*(4), 1640–1645. https://doi.org/10.1073/pnas.1314805111

Siame, B. A., Weerasuriya, Y., Wood, K., Ejeta, G., & Butler, L. G. (1993). Isolation of strigol, host plants germination stimulant for *Striga asiatica*, from of various crops in tropical and subtropical countries. *American Chemical Society*, *41*, 1486–1491. https://doi.org/10.1021/jf00033a025

Snowden, K. C., Simkin, A. J., Janssen, B. J., Templeton, K. R., Loucas, H. M., Simons, J. L., Karunairetnam, S., Gleave, A. P., Clark, D. G., & Klee, H. J. (2005). The decreased apical dominance1/*Petunia hybrida CAROTENOID CLEAVAGE DIOXYGENASE8* gene affects branch production and plays a role in leaf senescence, root growth, and flower development. *The Plant Cell.*, *17*, 746–759. https://doi.org/10.1105/tpc.104.027714

Sorefan, K., Booker, J., Haurogné, K., Goussot, M., Bainbridge, K., Foo, E., Chatfield, S., Ward, S., Beveridge, C., Rameau, C., & Leyser, O. (2003). MAX4 and RMS1 are orthologous dioxygenase-like genes that regulate shoot branching in Arabidopsis and pea. *Genes & Development*, *17*(12), 1469–1474. https://doi.org/10.1101/gad.256603

Stirnberg, P., Furner, I. J., & Leyser, H. M. O. (2007). MAX2 participates in an SCF complex which acts locally at the node to suppress shoot branching. *The Plant Journal*, *50*, 80–94. https://doi.org/10.1111/j.1365-313X.2007.03032.x

Stirnberg, P., van De Sande, K., & Leyser, H. O. (2002). MAX1 and MAX2 control shoot lateral branching in Arabidopsis.

Sun, H., Tao, J., Liu, S., Huang, S., Chen, S., Xie, X., Yoneyama, K., Zhang, Y., & Xu, G. (2014). Strigolactones are involved in phosphate- and nitrate-deficiency-induced root development and auxin transport in rice. *Journal of Experimental Botany*, *65*(22), 6735–6746. https://doi.org/10.1093/jxb/eru029

Tai, Z., Yin, X., Fang, Z., Shi, G., Lou, L., & Cai, Q. (2017). Exogenous GR24 alleviates cadmium toxicity by reducing cadmium uptake in switchgrass (*Panicum virgatum*) seedlings. *International Journal of Environmental Research and Public Health*, *14*(8), 852. https://doi.org/10.3390/ijerph14080852

Talhaoui, N., Taamalli, A., Gómez-Caravaca, A. M., Fernández-Gutiérrez, A., & Segura-Carretero, A. (2015). Phenolic compounds in olive leaves: Analytical determination, biotic and abiotic influence, and health benefits. *Food Research International*, *77*, 92–108. https://doi.org/10.1016/j.foodres.2015.09.011

Thula, S., Moturu, T. R., Salava, H., Balakhonova, V., Berka, M., Kerchev, P., Mishra, K. B., Nodzynski, T., & Simon, S. (2023). Strigolactones stimulate high light stress adaptation by modulating photosynthesis rate in Arabidopsis. *Journal of Plant Growth Regulation*, *42*(8), 4818–4833. https://doi.org/10.1007/s00344-022-10764-5

Toh, S., Kamiya, Y., Kawakami, N., Nambara, E., McCourt, P., & Tsuchiya, Y. (2012). Thermoinhibition uncovers a role for strigolactones in Arabidopsis seed germination. *Plant & Cell Physiology*, *53*(1), 107–117. https://doi.org/10.1093/pcp/pcr176

Tokunaga, T., Hayashi, H., & Akiyama, K. (2014). Medicaol, a strigolactone identified as a putative didehydro-orobancholisomer, from *Medicago truncatula*. *Phytochemistry*, *111*, 91–97. https://doi.org/10.1016/j.phytochem.2014.12.024

Trott, O., & Olson, A. J. (2010). AutoDock Vina: Improving the speed and accuracy of docking with a new scoring function, efficient optimization and multithreading. *Journal of Computational Chemistry*, *31*, 455–461. https://doi.org/10.1002/jcc.21334

Umehara, M., Cao, M., Akiyama, K., Akatsu, T., Seto, Y., Hanada, A., Li, W., Takeda-Kamiya, N., Morimoto, Y., & Yamaguchi, S. (2015). Structural requirements of strigolactones for shoot branching inhibition in rice and *Arabidopsis*. *Plant & Cell Physiology*, *56*(6), 1059–1072. https://doi.org/10.1093/pcp/pcv028

Umehara, M., Hanada, A., Yoshida, S., Akiyama, K., Arite, T., Takeda-Kamiya, N., Magome, H., Kamiya, Y., Shirasu, K., Yoneyama, K., Kyozuka, J., & Yamaguchi, S. (2008). Inhibition of shoot branching by new terpenoid plant hormones. *Nature*, *455*, 195–201. https://doi.org/10.1038/nature07272

Ünver, T., Wu, Z., Sterck, L., Turktas, M., Lohaus, R., Li, Z., Yang, M., He, L., Deng, T., Escalante, F. J., & Llorens, C. (2017). Genome of wild olive and the evolution of oil biosynthesis. *Proceedings of the National Academy of Sciences of the United States of America*, *114*(44), e9413–e9422.

Van Dingenen, J., De Keyser, A., Desmet, S., Clarysse, A., Beullens, S., Michiels, J., & Goormachtig, S. (2023). Strigolactones repress nodule development and senescence in pea. *The Plant Journal*, *116*(1), 7–22. https://doi.org/10.1111/tpj.16421

Vandesompele, J., De Preter, K., Pattyn, F., Poppe, B., Van Roy, N., De Paepe, A., & Speleman, F. (2002). Accurate normalization of real-time quantitative RT-PCR data by geometric averaging of multiple internal control genes. *Genome Biology*, *3*(7), research0034.1. https://doi.org/10.1186/gb-2002-3-7-research0034

Vogel, J. T., Walter, M. H., Giavalisco, P., Lytovchenko, A., Kohlen, W., Charnikhova, T., Simkin, A. J., Goulet, C., Strack, D., Bouwmeester, H. J., Fernie, A. R., & Klee, H. J. (2010). SlCCD7 controls strigolactone biosynthesis, shoot branching and mycorrhiza-induced apocarotenoid formation in tomato. *The Plant Journal*, *61*, 300–311. https://doi.org/10.1111/j.1365-313X.2009.04056.x

Voyiatzis, D. G. (1995). Dormancy and germination of olive embryos as affected by temperature. *Physiologia Plantarum*, *95*, 444–448. https://doi.org/10.1111/j.1399-3054.1995.tb00861.x

Wang, X., Li, Z., Shi, Y., Liu, Z., Zhang, X., Gong, Z., & Yang, S. (2023). Strigolactones promote plant freezing tolerance by releasing the WRKY41-mediated inhibition of CBF/DREB1 expression. *The EMBO Journal*, *42*(19), e112999. https://doi.org/10.15252/embj.2022112999

Waterhouse, A., Bertoni, M., Bienert, S., Studer, G., Tauriello, G., Gumienny, R., Heer, F. T., de Beer, T. A. P., Rempfer, C., Bordoli, L., Lepore, R., & Schwede, T. (2018). SWISS-MODEL: Homology modelling of protein structures and complexes. *Nucleic Acids Research*, *46*, 296–303. https://doi.org/10.1093/nar/gky427

Wen, C., Zhao, Q., Nie, J., Liu, G., Shen, L., Cheng, C., Xi, L., Ma, N., & Zhao, L. (2016). Physiological controls of chrysanthemum DgD27 gene expression in regulation of shoot branching. *Plant Cell Reports*, *35*, 1053–1070. https://doi.org/10.1007/s00299-016-1938-6

Xie, X., Yoneyama, K., Harada, Y., Fusegi, N., Yamada, Y., Ito, S., Yokota, T., Takeuchi, Y., & Yoneyama, K. (2009). Fabacyl acetate, a germination stimulant for root parasitic plants from *Pisum sativum*. *Phytochemistry*, *70*, 211–215. https://doi.org/10.1016/j.phytochem.2008.12.013

Yamada, Y., Furusawa, S., Nagasaka, S., Shimomura, K., Yamaguchi, S., & Umehara, M. (2014). Strigolactone signaling regulates rice leaf senescence in response to a phosphate deficiency. *Planta*, *240*, 399–408. https://doi.org/10.1007/s00425-014-2096-0

Yi, F., Song, A., Cheng, K., Liu, J., Wang, C., Shao, L., Wu, S., Wang, P., Zhu, J., Liang, Z., Chang, Y., Chu, Z., Cai, C., Zhang, X., Wang, P., Chen, A., Xu, J., Burritt, D. J., Herrera-Estrella, L., … Cai, Y. (2023). Strigolactones positively regulate Verticillium wilt resistance in cotton via crosstalk with other hormones. *Plant Physiology*, *192*(2), 945–966. https://doi.org/10.1093/plphys/kiad053

Yoneyama, K., Mori, N., Sato, T., Yoda, A., Xie, X., Okamoto, M., Iwanaga, M., Ohnishi, T., Nishiwaki, H., Asami, T., Yokota, T., Akiyama, K., Yoneyama, K., & Nomura, T. (2018). Conversion of carlactone to carlactonoic acid is a conserved function of MAX

1 homologs in strigolactone biosynthesis. *New Phytologist*, *218*(4), 1522–1533. https://doi.org/10.1111/nph.15055

Yoneyama, K., Xie, X., Yoneyama, K., Kisugi, T., Nomura, T., Nakatani, Y., Akiyama, K., & McErlean, C. S. P. (2018). Which are the major players, canonical or non-canonical strigolactones? *Journal of Experimental Botany*, *69*(9), 2231–2239. https://doi.org/10.1093/jxb/ery090

Yu, C., Chen, W., Wang, Z., & Lou, H. (2021). Comparative proteomic analysis of tomato (*Solanum lycopersicum* L.) shoots reveals crosstalk between strigolactone and auxin. *Genomics*, *113*(5), 3163–3173. https://doi.org/10.1016/j.ygeno.2021.07.009

Zhang, X., Zhang, L., Ma, C., Su, M., Wang, J., Zheng, S., & Zhang, T. (2022). Exogenous strigolactones alleviate the photosynthetic inhibition and oxidative damage of cucumber seedlings under salt stress. *Scientia Horticulturae*, *297*, 110962. https://doi.org/10.1016/j.scienta.2022.110962

Zhang, Y., van Dijk, A. D. J., Scaffidi, A., Flematti, G. R., Hofmann, M., Charnikhova, T., Verstappen, F., Hepworth, J., van der Krol, S., Leyser, O., Smith, S. M., Zwanenburg, B., al-Babili, S., Ruyter-Spira, C., & Bouwmeester, H. J. (2014). Rice cytochrome P450 MAX1 homologs catalyze distinct steps in strigolactone biosynthesis. *Nature Chemical Biology*, *10*(12), 1028–1033. https://doi.org/10.1038/nchembio.1660

Zheng, K., Wang, X., Weighill, D. A., Guo, H., Xie, M., Yang, Y., Yang, J., Wang, S., Jacobson, D. A., Guo, H., Muchero, W., Tuskan, G. A., & Chen, J. (2016). Characterization of DWARF14 genes in Populus. *Scientific Reports*, *6*, 1–11. https://doi.org/10.1038/srep21593

Zheng, X., Li, Y., Xi, X., Ma, C., Sun, Z., Yang, X., Li, X., Tian, Y., & Wang, C. (2021). Exogenous Strigolactones alleviate KCl stress by regulating photosynthesis, ROS migration and ion transport in *Malus hupehensis* Rehd. *Plant Physiology and Biochemistry*, *159*, 113–122. https://doi.org/10.1016/j.plaphy.2020.12.015

Zhou, F., Lin, Q., Zhu, L., Ren, Y., Zhou, K., Shabek, N., Wu, F., Mao, H., Dong, W., Gan, L., Ma, W., Gao, H., Chen, J., Yang, C., Wang, D., Tan, J., Zhang, X., Guo, X., Wang, J., … Wan, J. (2013). D14-SCFD3-dependent degradation of D53 regulates strigolactone signalling. *Nature*, *504*, 406–410. https://doi.org/10.1038/nature12878

Zhou, X., Tan, Z., Zhou, Y., Guo, S., Sang, T., Wang, Y., & Shu, S. (2022). Physiological mechanism of strigolactone enhancing tolerance to low light stress in cucumber seedlings. *BMC Plant Biology*, *22*(1), 30. https://doi.org/10.1186/s12870-021-03414-7

Zohary, D., Hopf, M., & Weiss, E. (2012). *Domestication of plants in the Old World* (4th ed.) (p. 251). Oxford University Press, United States.

SUPPORTING INFORMATION

Additional supporting information can be found online in the Supporting Information section at the end of this article.

How to cite this article: Özbilen, A., Sezer, F., & Taşkin, K. M. (2024). Identification and expression of strigolactone biosynthesis and signaling genes and the in vitro effects of strigolactones in olive (*Olea europaea* L.). *Plant Direct*, *8*(2), e568. https://doi.org/10.1002/pld3.568